NAVAL POSTGRADUATE SCHOOL
Monterey, California

THESIS

**INITIAL STUDIES OF STRUCTURAL COUPLING
EFFECTS FOR A TROLLEY/RRDF INTERFACE**

by

Chong-Ann Teh

March 2003

Thesis Advisor: Fotis A. Papoulias

Approved for public release; distribution is unlimited

THIS PAGE INTENTIONALLY LEFT BLANK

REPORT DOCUMENTATION PAGE	*Form Approved OMB No. 0704-0188*

Public reporting burden for this collection of information is estimated to average 1 hour per response, including the time for reviewing instruction, searching existing data sources, gathering and maintaining the data needed, and completing and reviewing the collection of information. Send comments regarding this burden estimate or any other aspect of this collection of information, including suggestions for reducing this burden, to Washington headquarters Services, Directorate for Information Operations and Reports, 1215 Jefferson Davis Highway, Suite 1204, Arlington, VA 22202-4302, and to the Office of Management and Budget, Paperwork Reduction Project (0704-0188) Washington DC 20503.

1. AGENCY USE ONLY *(Leave blank)*	2. REPORT DATE March 2003	3. REPORT TYPE AND DATES COVERED Master's Thesis	
4. TITLE AND SUBTITLE: Initial Studies of Structure Coupling Effects for a Trolley/RRDF Interface		5. FUNDING NUMBERS	
6. AUTHOR(S) Chong-Ann Teh			
7. PERFORMING ORGANIZATION NAME(S) AND ADDRESS(ES) Naval Postgraduate School Monterey, CA 93943-5000		8. PERFORMING ORGANIZATION REPORT NUMBER	
9. SPONSORING /MONITORING AGENCY NAME(S) AND ADDRESS(ES) N/A		10. SPONSORING/MONITORING AGENCY REPORT NUMBER	

11. SUPPLEMENTARY NOTES The views expressed in this thesis are those of the author and do not reflect the official policy or position of the Department of Defense or the U.S. Government.

12a. DISTRIBUTION / AVAILABILITY STATEMENT Approved for public release; distribution is unlimited	12b. DISTRIBUTION CODE

13. ABSTRACT *(maximum 200 words)*

The purpose of this thesis is to lay the foundation for analyzing structural coupling effects for a proposed trolley interface between a ship and a roll-on roll-off discharge facility (RRDF). Such a facility could allow heavy cargo transfer at higher sea states. Previous studies have analyzed motions assuming that there is no structural coupling between the trolley and the RRDF. A mathematical model that incorporates structural coupling is developed using the principle of virtual work. In order to assess the degree of necessity for the proposed model we conduct a systematic series of numerical experiments. In these calculations we model the trolley through a generalized stiffness coefficient and assess its influence on RRDF motions. It is shown that modeling of structural coupling may be necessary depending on the relative order of magnitude of trolley structural rigidity and trolley placement

14. SUBJECT TERMS Structure Coupling, Trolley, RRDF, Assumed Modes, Virtual Work	15. NUMBER OF PAGES 77
	16. PRICE CODE

17. SECURITY CLASSIFICATION OF REPORT Unclassified	18. SECURITY CLASSIFICATION OF THIS PAGE Unclassified	19. SECURITY CLASSIFICATION OF ABSTRACT Unclassified	20. LIMITATION OF ABSTRACT UL

THIS PAGE INTENTIONALLY LEFT BLANK

INITIAL STUDIES OF STRUCTURAL COUPLING EFFECTS FOR A TROLLEY/RRDF INTERFACE

Chong-Ann Teh
Major, Republic of Singapore Navy
B.S. (Mech. Eng.), National University of Singapore, 1994

Submitted in partial fulfillment of the
requirements for the degree of

MASTER OF SCIENCE IN MECHANICAL ENGINEERING

from the

NAVAL POSTGRADUATE SCHOOL
March 2003

Author: Chong-Ann Teh

Approved by: Fotis A. Papoulias
      Thesis Advisor

      Young Kwon
      Chairman, Department of Mechanical Engineering

THIS PAGE INTENTIONALLY LEFT BLANK

ABSTRACT

The purpose of this thesis is to lay the foundation for analyzing structural coupling effects for a proposed trolley interface between a ship and a roll-on roll-off discharge facility (RRDF). Such a facility could allow heavy cargo transfer at higher sea states. Previous studies have analyzed motions assuming that there is no structural coupling between the trolley and the RRDF. A mathematical model that incorporates structural coupling is developed using the principle of virtual work. In order to assess the degree of necessity for the proposed model we conduct a systematic series of numerical experiments. In these calculations we model the trolley through a generalized stiffness coefficient and assess its influence on RRDF motions. It is shown that modeling of structural coupling may be necessary depending on the relative order of magnitude of trolley structural rigidity and trolley placement.

THIS PAGE INTENTIONALLY LEFT BLANK

TABLE OF CONTENTS

THIS PAGE INTENTIONALLY LEFT BLANK

LIST OF FIGURES

ACKNOWLEDGMENTS

I would like to thank the following people for making this thesis a reality:

My wife, Yvonne, for her understanding and support,

My thesis advisor, Professor Papoulias, for his guidance,

The September '01 batch that provided the encouragements,

Pam Silva, for her smile and assistance, and

ME students at NPS, that help in one way or another.

THIS PAGE INTENTIONALLY LEFT BLANK

I.   INTRODUCTION

One of the salient features of the United States Military approach to 21st Century Joint Warfare is **Maneuver Warfare.** Maneuver warfare seeks to attack adversary vulnerabilities from a position of advantage through the synchronized application of movement and fires.   This is one of the reasons for the creation of the Naval Expeditionary Strike Group (NESG). Current NESG comprises of several classes of ships such as the LMSR, CAPE-D, CAPE-H and CAPE-T to deliver the necessary military equipment and stores to support its mission. In situation where a friendly port is available close to the objective, these ships can unload their payload through the port facilities. However there are situations where a friendly port is not in close proximity resulting in a need to perform at sea transfer of the payload. This involves ship-to-ship transfer of payload from these large ships to smaller crafts that subsequently delivers the payload to shore.

Current ship-to-ship transfer involves a ramp interface for heavy equipment such as the M1A1 main battle tanks. This technique is limited to operations at sea-state 3 due to excessive torsional stresses on the ramp when two main battle tanks are located in the proximity of the middle of the ramp. A previous study on a new method of transferring cargo based on the use of a trolley-rail interface shows potential advantages in the reduction of torsional stresses and weight. This thesis lays the foundation for analyzing structural coupling effects for the proposed trolley interface between a ship and a roll-on roll-off discharge facility (RRDF), and determines the necessity for modeling of structural coupling depending on the relative order of magnitude of trolley structural rigidity and trolley placement.

THIS PAGE INTENTIONALLY LEFT BLANK

II. BACKGROUND INFORMATION

Amphibious operations conducted by the US military involves large amount of equipment and stores that needs to be unloaded near to the objective. These equipment and stores are usually kept in prepositioned ships at various parts of the world such that the response time of the forces can be greatly reduced. However, the current mode of operations requires these prepositioned ships to unload their cargo either at nearby port facilities, which is the preferred option, or in the event that such ports are not available, go right up to within 2 nautical mile of the beach to unload their cargo onto barges or small crafts that ferry these equipment and stores ashore. There are two main problems with the current mode of operation. First of all, the number of available ports for the prepositioned ships to unload their cargo is severely limited. Secondly, the number of beaches that would enable these large prepositioned ships to go right near and unload their cargo on the beaches is also very limited. The reason for this is that the transfer of cargo from the preposition ship to the barge can only be conducted at sea-state three and below to prevent excessive torsional stress on the ships' ramp when unloading heavy equipment such as the 68-tonnes M1A1 main battle tank [Ref 1]. These problems, coupled with the fact that such operations results in extended time when the amphibious force needs to defend the logistic operations meant that a better way has to be developed. This is the main driver for the new Trolley-Rail system proposed by Advanced Design Consulting Inc, which aims to enable the transferring of cargo between ships at higher sea states. Studies on the response of the proposed system under seaway has yield positive results indicating that the system should be able to achieve the required transfer rate at higher sea states [Ref 2].

THIS PAGE INTENTIONALLY LEFT BLANK

III. MODELING

A. TROLLEY-RAIL MODEL

The Trolley-Rail system proposed by Advance Design Consulting Inc. essentially comprise of two parallel rails that runs from one ship to the other ship. The trolley (or platform) traverses along the two rails via attached wheels to transport equipment and stores from the prepositioned ships to shuttle ships that ferry these cargo ashore. For the model, the other ship is the Roll-on Roll-off Discharge Facility (RRDF). The RRDF is made up of a number of interconnected modules which serves as the platform to support the rails running from the ship, and to facilitate the movement of the equipment and stores to the shuttle ships. A schematic of the Trolley-Rail system is given shown in Figure (1) while the three-dimensional model is shown in Figure (2), and the RRDF is shown in Figure (3):
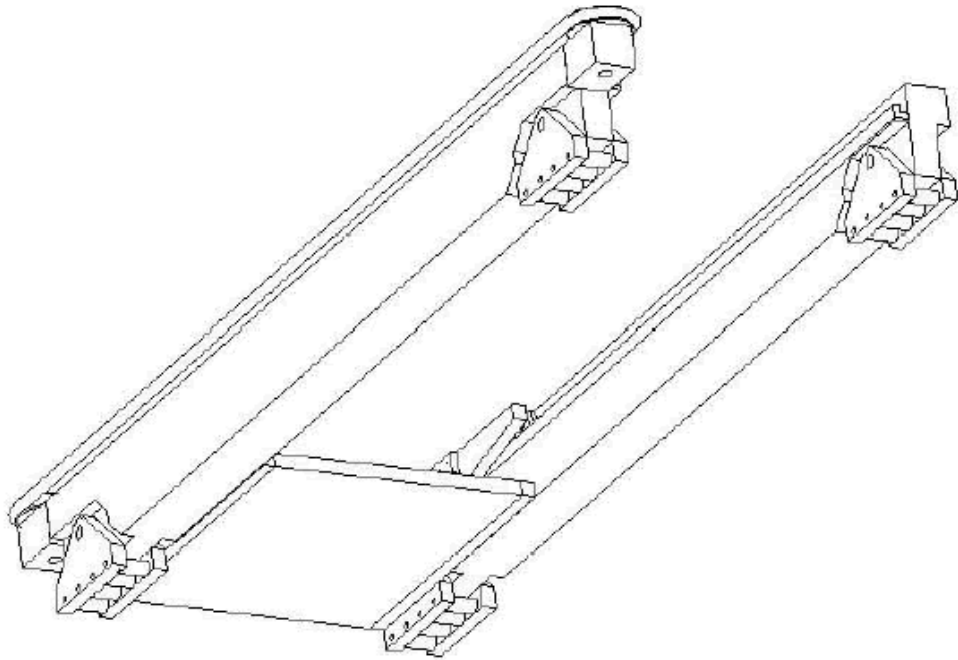
Figure 1.   Schematic of Trolley-Rail System
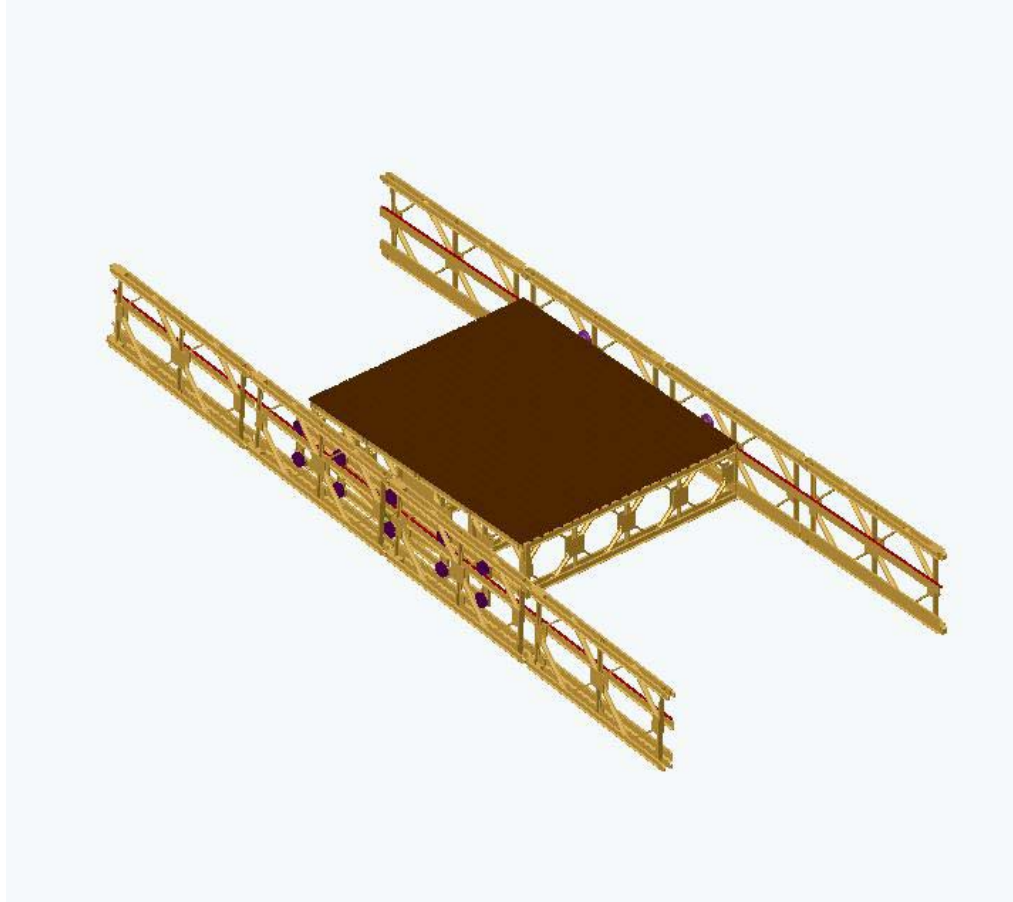
Figure 2.   3-D model of Trolley-Rail System
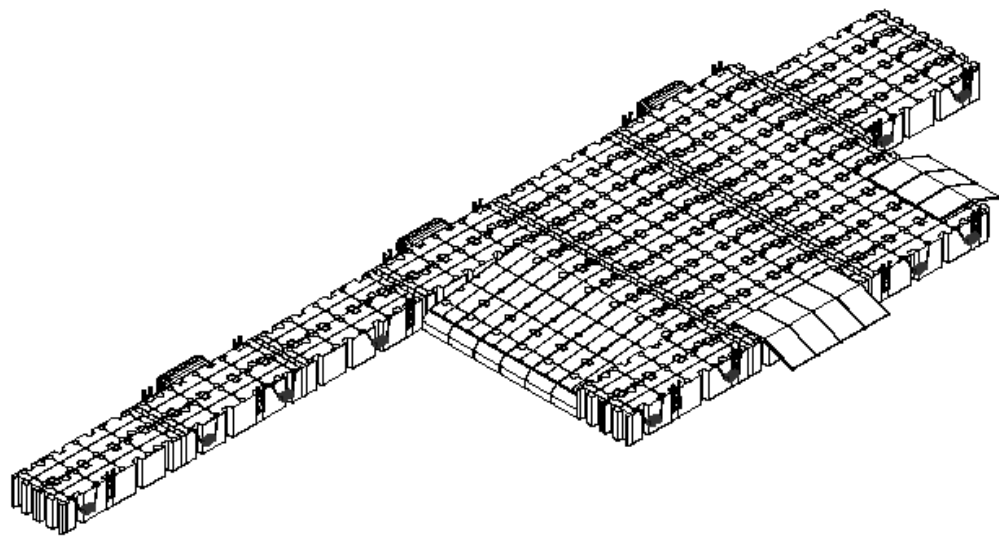
Figure 3.   Schematic of Roll-on Roll-off Discharge Facility (RRDF)

The rails are each modeled as a beam structure. This is a good model as the length of each rail is very much greater than its width and thickness. The rails are assumed to be pinned at the ship's end while the other end is free. Each rail is connected by a spring, dashpot and actuator to the RRDF to simulate potential active control mechanism. The RRDF is connected by a spring and dashpot to the ground to simulate the motion of the seaway [Ref 3]. The trolley will effect structural coupling on the two rails and this is being modeled as a spring and a dashpot. Two lump masses are also attached at the trolley interface with the two rails to account for the cargo loading on the trolley. A schematic of the model is shown in Figure 3.
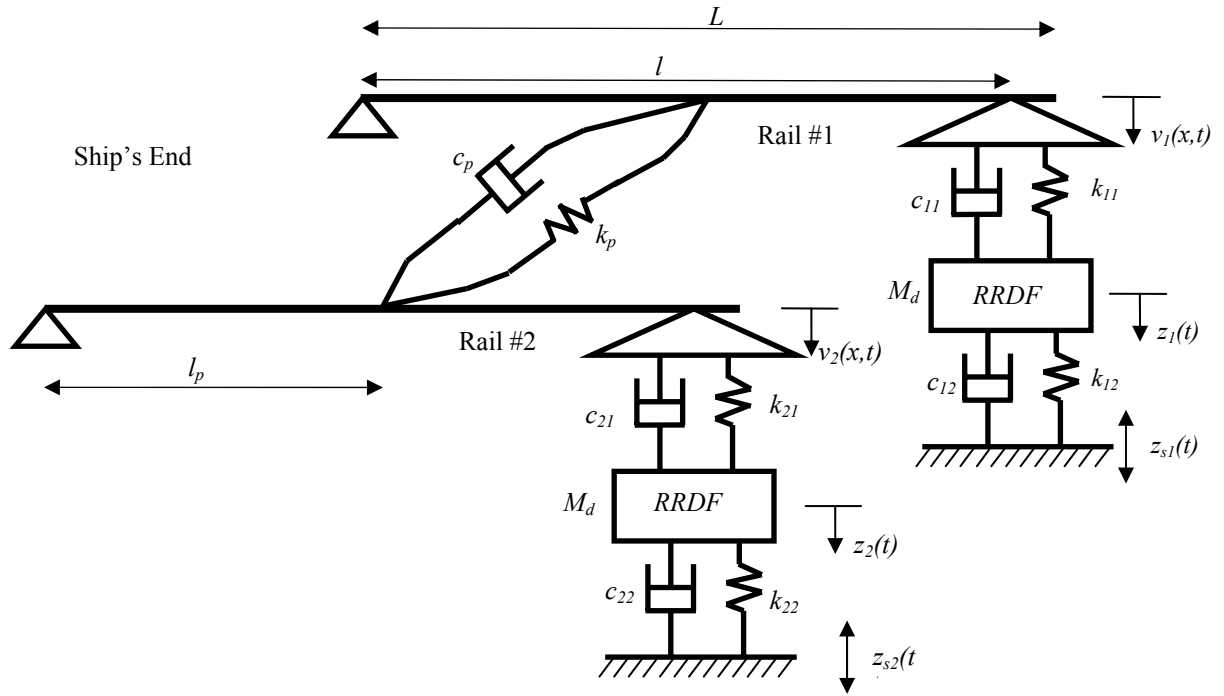
Figure 4.   Model of Trolley-Rail System

The parameters for the model are given as follows:

L = length of each Rail

l = length between supports along Rail

l_p = length of trolley

p = distance along the beam from ship end to the center line of the trolley

M_d = mass contribution of RRDF at the support location of the free end of beam

k_{11} = stiffness ratio between Rail # 1 and the RRDF

c_{11} = proportional damping ratio between Rail #1 and the RRDF

k_{12} = stiffness ratio between the RRDF and the ground at Rail # 1 locality

c_{12} = proportional damping ratio between the RRDF and the ground at Rail # 1 locality

k_{21} = stiffness ratio between Rail # 2 and the RRDF

c_{21} = proportional damping ratio between Rail #2 and the RRDF

k_{22} = stiffness ratio between the RRDF and the ground at Rail # 2 locality

c_{22} = proportional damping ratio between the RRDF and the ground at Rail # 2 locality

$v_1(x,t)$ = transverse deflection of Rail #1

$z_1(t)$ = vertical displacement of RRDF at locality of Rail #1

$z_{s1}(t)$ = vertical displacement of the sea wave at locality of Rail #1

$v_2(x,t)$ = transverse deflection of Rail #2

$z_2(t)$ = vertical displacement of RRDF at locality of Rail #2

$z_{s2}(t)$ = vertical displacement of the sea wave at locality of Rail #2

B.   DERIVATION OF MATHEMATICAL MODEL

1.   Equation of Motion

Having developed the schematic of the model, the next step is to derive the equations of motion for the model. Lagrange equation was employed for this purpose. First of all, the kinetic energy of the system is given by

$$T = \frac{1}{2}\int_0^L \rho A \left(\frac{\partial v_1}{\partial t}\right)^2 dx + \frac{1}{2}\int_0^L \rho A \left(\frac{\partial v_2}{\partial t}\right)^2 dx + \frac{1}{2}M_d \left(\frac{\ddot{z}_1 - \ddot{z}_2}{2}\right) + \frac{1}{2}J_d \dot{\theta}^2$$

$$+ \frac{1}{2}\left(\frac{M_p}{2}\right)\left[\dot{v}_1(p,t)\right]^2 + \frac{1}{2}\left(\frac{M_p}{2}\right)\left[\dot{v}_2(p,t)\right]^2$$

Working on the premise of small angles, the angular velocity of the RRDF may be approximated by,

$$\dot{\theta} = \frac{\dot{z}_1 - \dot{z}_2}{w}$$

where w is the width of the RRDF.

Hence, the kinetic energy is given by

$$T = \frac{1}{2}\int_0^L \rho A \left(\frac{\partial v_1}{\partial t}\right)^2 dx + \frac{1}{2}\int_0^L \rho A \left(\frac{\partial v_2}{\partial t}\right)^2 dx + \frac{1}{2}M_d \left(\frac{\ddot{z}_1 - \ddot{z}_2}{2}\right) + \frac{1}{2w}J_d \left(\dot{z}_1 - \dot{z}_2\right)^2$$

$$+ \frac{1}{2}\left(\frac{M_p}{2}\right)\left[\dot{v}_1(p,t)\right]^2 + \frac{1}{2}\left(\frac{M_p}{2}\right)\left[\dot{v}_2(p,t)\right]^2$$

The strain energy of the system is given by

$$U = \frac{1}{2}\int_0^L EI \left(\frac{\partial^2 v_1}{\partial x^2}\right)^2 dx + \frac{1}{2}k_{11}\left[v_1(l,t) - z_1\right]^2 + \frac{1}{2}k_{12}z_1^2$$

$$+ \frac{1}{2}\int_0^L EI \left(\frac{\partial^2 v_2}{\partial x^2}\right)^2 dx + \frac{1}{2}k_{21}\left[v_2(l,t) - z_2\right]^2 + \frac{1}{2}k_{22}z_2^2$$

$$+ \frac{1}{2}k_p \left[v_1(p,t) - v_2(p,t)\right]^2$$

9

For the rails which are modeled as beam structures, the assumed mode method is employed to approximate the transverse vibration of each beam, given by

$$v_1(x,t) = \sum_{i=1}^{N} \psi_i(x)\alpha_i(t)$$

$$v_2(x,t) = \sum_{i=1}^{N} \psi_i(x)\beta_i(t)$$

where $\psi_i(x)$ is the assumed modes that satisfies the geometric boundary conditions of the beam and N is the number of modes that was used in the computation.

To reduce the mathematical complexity, indicial notations are utilized to represent the transverse deflection of the beam. Therefore the transverse deflection of each beam is given as

$$v_1(x,t) = \psi_i \alpha_i$$

$$v_2(x,t) = \psi_i \beta_i$$

where the subscript i represents a summation from 1 to N.

Hence, the kinetic energy of the system is represented in the form,

$$T = \frac{1}{2} \int_0^L \rho A \{\psi_i(x)\dot{\alpha}_i(t)\}\{\psi_j(x)\dot{\alpha}_j(t)\} dx$$

$$+ \frac{1}{2} \int_0^L \rho A \{\psi_i(x)\dot{\beta}_i(t)\}\{\psi_j(x)\dot{\beta}_j(t)\} dx$$

$$+ \frac{1}{8} M_d (\ddot{z}_1 - \ddot{z}_2)^2 + \frac{1}{2w^2} J_d (\dot{z}_1 - \dot{z}_2)^2$$

$$+ \frac{1}{4} M_p \left[\{\psi_i(p)\dot{\alpha}_i(t)\}\{\psi_j(p)\dot{\alpha}_j(t)\} \right] + \frac{1}{4} M_p \left[\{\psi_i(p)\dot{\beta}_i(t)\}\{\psi_j(p)\dot{\beta}_j(t)\} \right]$$

10

while the potential energy of the system is represented in the form,

$$U = \frac{1}{2}\int_0^L EI\{\psi_i''(x)\alpha_i(t)\}\{\psi_j''(x)\alpha_j(t)\}\,dx + \frac{1}{2}k_{11}[\psi_i(l)\alpha_i(t) - z_1]^2 + \frac{1}{2}k_{12}z_1^2$$

$$+ \frac{1}{2}\int_0^L EI\{\psi_i''(x)\beta_i(t)\}\{\psi_j''(x)\beta_j(t)\}\,dx + \frac{1}{2}k_{21}[\psi_i(l)\beta_i(t) - z_2]^2 + \frac{1}{2}k_{22}z_2^2$$

$$+ \frac{1}{2}k_p[\psi_i(p)\alpha_i(t) - \psi_i(p)\beta_i(t)]^2$$

Applying the Lagrange equation,

$$\frac{d}{dt}\left(\frac{\partial T}{\partial \dot{q}_i}\right) - \frac{\partial T}{\partial q_i} + \frac{\partial U}{\partial q_i} - Q_i = 0$$

the generalized coordinates for the model are chosen as,

$$\tilde{q} = \begin{bmatrix} z_1 & z_2 & \alpha_1 & \alpha_2 & \cdots & \alpha_N & \beta_1 & \beta_2 & \cdots & \beta_N \end{bmatrix}^T$$

The various differentials in the Lagrange equation are given by

$$\frac{d}{dt}\left(\frac{\partial T}{\partial \dot{z}_1}\right) = \left(\frac{1}{2}M_d + \frac{1}{w^2}J_d\right)(\ddot{z}_1 - \ddot{z}_2)$$

$$\frac{d}{dt}\left(\frac{\partial T}{\partial \dot{z}_2}\right) = \left(\frac{1}{2}M_d + \frac{1}{w^2}J_d\right)(\ddot{z}_2 - \ddot{z}_1)$$

$$\frac{d}{dt}\left(\frac{\partial T}{\partial \dot{\alpha}_i}\right) = \left\{\int_0^L \rho A\left[\psi_i(x)\psi_j(x)\right]dx\right\}\ddot{\alpha}_j(t) + \frac{1}{2}M_p\psi_i(p)\psi_j(p)\ddot{\alpha}_j(t)$$

$$\frac{d}{dt}\left(\frac{\partial T}{\partial \dot{\beta}_i}\right) = \left\{\int_0^L \rho A\left[\psi_i(x)\psi_j(x)\right]dx\right\}\ddot{\beta}_j(t) + \frac{1}{2}M_p\psi_i(p)\psi_j(p)\ddot{\beta}_j(t)$$

$$\frac{\partial T}{\partial z_1} = \frac{\partial T}{\partial z_2} = \frac{\partial T}{\partial \alpha_i} = \frac{\partial T}{\partial \beta_i} = 0$$

$$\frac{\partial U}{\partial z_1} = -k_{11}\left[\psi_i(x)\alpha_i(t) - z_1\right] + k_{12}z_1$$

$$= \left(k_{11} + k_{12}\right)z_1 - k_{11}\psi_i(l)\alpha_i(t)$$

$$\frac{\partial U}{\partial z_2} = \left(k_{21} + k_{22}\right)z_2 - k_{21}\psi_i(l)\beta_i(t)$$

$$\frac{\partial U}{\partial \alpha_i} = \left\{\int_0^L EI\left[\psi_i^{"}(x)\psi_j^{"}(x)\right]dx\right\}\alpha_j(t)$$

$$+ k_{11}\left[\psi_i(x)\alpha_i(t) - z_1\right]\psi_j(l)$$

$$+ k_p\left[\psi_i(p)\alpha_i(t) - \psi_j(p)\beta_j(t)\right]\psi_j(p)$$

$$\frac{\partial U}{\partial \beta_i} = \left\{\int_0^L EI\left[\psi_i^{"}(x)\psi_j^{"}(x)\right]dx\right\}\beta_j(t)$$

$$+ k_{21}\left[\psi_i(x)\beta_i(t) - z_2\right]\psi_j(l)$$

$$- k_p\left[\psi_i(p)\alpha_i(t) - \psi_j(p)\beta_j(t)\right]\psi_j(p)$$

The principle of virtual work is used to determine the generalized force $Q_{i,}$. The RRDF and the beams are assumed to have very small movements as follows:

δz_1, δz_2, $\delta v_1(l,t)$, and $\delta v_2(l,t)$ at location $x = l$

$\delta v_1(p,t)$, and $\delta v_2(p,t)$ at location $x = p$

The virtual work done due to dampers resisting force is then given by

$$\delta W^d = -c_{12}\dot{z}_1\delta z_1 - c_{11}\left[\dot{z}_1 - \dot{v}_1(l,t)\right]\left[\delta z_1 - \delta v_1(l,t)\right]$$

$$- c_{22}\dot{z}_2\delta z_2 - c_{21}\left[\dot{z}_2 - \dot{v}_2(l,t)\right]\left[\delta z_2 - \delta v_2(l,t)\right]$$

$$- c_p\left[\dot{v}_1(p,t) - \dot{v}_2(p,t)\right]\left[\delta v_1(p,t) - \delta v_2(p,t)\right]$$

$$\therefore \delta W^d = \left[-(c_{12}+c_{11})\dot{z}_1 + c_{11}\psi_i(l)\dot{\alpha}_i(t)\right]\delta z_1$$

$$+ \left[-(c_{22}+c_{21})\dot{z}_2 + c_{21}\psi_i(l)\dot{\beta}_i(t)\right]\delta z_2$$

$$+ \left[c_{11}\dot{z}_1\psi_i(l) - c_{11}\psi_i(l)\psi_j(l)\dot{\alpha}_i(t)\right]\delta\alpha_i$$

$$+ \left[-c_p\left\{\psi_i(p)\dot{\alpha}_i(t) - \psi_j(p)\dot{\beta}_j(t)\right\}\psi_j(p)\right]\delta\alpha_i$$

$$+ \left[c_{21}\dot{z}_2\psi_i(l) - c_{21}\psi_i(l)\psi_j(l)\dot{\beta}_i(t)\right]\delta\beta_i$$

$$+ \left[c_p\left\{\psi_i(p)\dot{\alpha}_i(t) - \psi_j(p)\dot{\beta}_j(t)\right\}\psi_j(p)\right]\delta\beta_i$$

Hence, the generalize forces due to the dampers are given by

$$Q_{z_1}^d = -\left(c_{12}+c_{11}\right)\dot{z}_1 + c_{11}\psi_i(l)\dot{\alpha}_i(t)$$

$$Q_{z_2}^d = -\left(c_{22}+c_{21}\right)\dot{z}_2 + c_{21}\psi_i(l)\dot{\beta}_i(t)$$

$$Q_{\alpha_i}^d = c_{11}\psi_i(l)\dot{z}_1 + \left[-c_{11}\psi_i(l)\psi_j(l) + c_p\psi_i(p)\psi_j(p)\right]\dot{\alpha}_j(t) - \left[c_p\psi_i(p)\psi_j(p)\right]\dot{\beta}_j(t)$$

$$Q_{\beta_i}^d = c_{21}\psi_i(l)\dot{z}_2 - \left[c_p\psi_i(p)\psi_j(p)\right]\dot{\alpha}_j(t) + \left[-c_{21}\psi_i(l)\psi_j(l) + c_p\psi_i(p)\psi_j(p)\right]\dot{\beta}_j(t)$$

13

For the external forces, the virtual work done is given by

$$\delta W^f = -M_d \left(\frac{\ddot{z}_{s1} - \ddot{z}_{s2}}{2} \right)\left(\frac{\delta z_1 - \delta z_2}{2} \right) - J_d \ddot{\theta} \left(\frac{\delta z_1 - \delta z_2}{w} \right)$$

$$-\int_0^L \rho A \frac{x}{l} \ddot{z}_{s1}(t) \delta v_1(x,t) dx$$

$$-\int_0^L \rho A \frac{x}{l} \ddot{z}_{s2}(t) \delta v_2(x,t) dx$$

$$\therefore \delta W^f = -\left(\frac{1}{4} M_d + \frac{1}{w^2} J_d \right)(\ddot{z}_{s1} - \ddot{z}_{s2}) \delta z_1$$

$$+ \left(\frac{1}{4} M_d + \frac{1}{w^2} J_d \right)(\ddot{z}_{s1} - \ddot{z}_{s2}) \delta z_2$$

$$- \left[\int_0^L \rho A \frac{x}{l} \ddot{z}_{s1}(t) \psi_i(x) dx \right] \delta \alpha_i$$

$$- \left[\int_0^L \rho A \frac{x}{l} \ddot{z}_{s2}(t) \psi_i(x) dx \right] \delta \beta_i$$

Hence, the generalized forces due to external forces are given by

$$Q_{z_1}^f = -\left(\frac{1}{4} M_d + \frac{1}{w^2} J_d \right)(\ddot{z}_{s1} - \ddot{z}_{s2})$$

$$Q_{z_2}^f = \left(\frac{1}{4} M_d + \frac{1}{w^2} J_d \right)(\ddot{z}_{s1} - \ddot{z}_{s2})$$

$$Q_{\alpha_i}^f = -\left[\int_0^L \rho A \frac{x}{l} \psi_i(x) dx \right] \ddot{z}_{s1}(t)$$

$$Q_{\beta_i}^f = -\left[\int_0^L \rho A \frac{x}{l} \psi_i(x) dx \right] \ddot{z}_{s2}(t)$$

14

Finally, the equation of motion in generalized coordinates form is given as

$$[M]\{\ddot{q}\}+[C]\{\dot{q}\}+[K]\{q\}=\{Q\}$$

whereby the matrices are given by

$$[M]=\begin{pmatrix} M_R & -M_R & 0_{(2\times 2N)} \\ -M_R & M_R & & \\ 0_{(2N\times 2)} & & \hat{M}_{\alpha(N\times N)} & \\ & & & \hat{M}_{\beta(N\times N)} \end{pmatrix}$$

where $M_R=\left(\dfrac{1}{4}M_d+\dfrac{1}{w^2}J_d\right)$

$$\hat{M}_{\alpha_{ij}}=\hat{M}_{\beta_{ij}}=\int_0^L \rho A\psi_i(x)\psi_j(x)dx+\frac{1}{2}M_p\psi_i(p)\psi_j(p)$$

$$[K]=\begin{pmatrix} (k_{11}+k_{12}) & 0 & -k_{11}\psi_i(l)_{(1\times N)} & 0_{(1\times N)} \\ 0 & (k_{11}+k_{12}) & 0_{(1\times N)} & -k_{21}\psi_i(l)_{(1\times N)} \\ -k_{11}\psi_i(l)_{(N\times 1)} & 0_{(N\times 1)} & \hat{K}_{\alpha(N\times N)} & \hat{K}_{\alpha\beta(N\times N)} \\ 0_{(N\times 1)} & -k_{21}\psi_i(l)_{(N\times 1)} & \hat{K}_{\alpha\beta(N\times N)} & \hat{K}_{\beta(N\times N)} \end{pmatrix}$$

where $\hat{K}_{\alpha_{ij}}=\int_0^L EI\psi_i''(x)\psi_j''(x)dx+k_{11}\psi_i(l)\psi_j(l)+k_p\psi_i(p)\psi_j(p)$

$\hat{K}_{\alpha_{ij}}=\int_0^L EI\psi_i''(x)\psi_j''(x)dx+k_{21}\psi_i(l)\psi_j(l)+k_p\psi_i(p)\psi_j(p)$

$\hat{K}_{\alpha\beta_{ij}}=-k_p\psi_i(p)\psi_j(p)$

$$[C] = \begin{pmatrix} (c_{12}+c_{11}) & 0 & c_{11}\psi_i(l)_{(1\times N)} & 0_{(1\times N)} \\ 0 & -(c_{22}+c_{21}) & 0_{(1\times N)} & c_{21}\psi_i(l)_{(1\times N)} \\ c_{11}\psi_i(l)_{(N\times 1)} & 0_{(N\times 1)} & \hat{C}_{\alpha_{(N\times N)}} & \hat{C}_{\alpha\beta_{(N\times N)}} \\ 0_{(N\times 1)} & c_{21}\psi_i(l)_{(N\times 1)} & \hat{C}_{\alpha\beta_{(N\times N)}} & \hat{C}_{\beta_{(N\times N)}} \end{pmatrix}$$

where $\hat{C}_{\alpha_{ij}} = -c_{11}\psi_i(l)\psi_j(l) + c_p\psi_i(p)\psi_j(p)$

$$\hat{C}_{\alpha_{ij}} = -c_{21}\psi_i(l)\psi_j(l) + c_p\psi_i(p)\psi_j(p)$$

$$\hat{C}_{\alpha\beta_{ij}} = -c_p\psi_i(p)\psi_j(p)$$

$$\{Q\} = \begin{Bmatrix} -M_R(\ddot{z}_{s1}-\ddot{z}_{s2}) \\ M_R(\ddot{z}_{s1}-\ddot{z}_{s2}) \\ \hat{Q}\ddot{z}_{s1_{(N\times 1)}} \\ \hat{Q}\ddot{z}_{s2_{(N\times 1)}} \end{Bmatrix}$$

where $\hat{Q}_{ij} = -\int_0^L \rho A \frac{x}{l}\psi_i(x)dx$

2. Assumed Modes for Beam

The assumed modes, which satisfy the geometric boundary conditions, need to be used to calculate the generalized mass, damping, stiffness and force matrices. The general solution of the beam is given by [Ref 4]

$$y = A\cosh\beta x + B\sinh\beta x + C\cos\beta x + D\sin\beta x$$

The boundary conditions are:

At $x = 0$ $\begin{cases} y = 0 \\ \dfrac{d^2 y}{dx^2} = 0 \qquad (M = 0) \end{cases}$

At $x = L$ $\begin{cases} \dfrac{d^2 y}{dx^2} = 0 \qquad (M = 0) \\ \dfrac{d^3 y}{dx^3} = 0 \qquad (V = 0) \end{cases}$

$$\left. \begin{aligned} (y)_{x=0} &= A + C = 0 \qquad\qquad \Rightarrow A = -C \\ \left(\frac{d^2 y}{dx^2}\right)_{x=0} &= \beta(A - C) = 0 \quad \Rightarrow A = C \end{aligned} \right\} A = C = 0$$

$$\left(\frac{d^2 y}{dx^2}\right)_{x=L} = \beta^2 \left(B \sinh(\beta L) - D \sin(\beta L) \right) = 0$$

$$\Rightarrow B = \frac{\sin(\beta L)}{\sinh(\beta L)} D$$

$$\left(\frac{d^3 y}{dx^3}\right)_{x=L} = \beta^3 \left(B \cosh(\beta L) - D \cos(\beta L) \right) = 0$$

$$\Rightarrow B = \frac{\cos(\beta L)}{\cosh(\beta L)} D$$

$$\frac{\sin(\beta L)}{\sinh(\beta L)} = \frac{\cos(\beta L)}{\cosh(\beta L)}$$

$$\Rightarrow \tan(\beta L) = \tanh(\beta L)$$

$$\text{and } y_i = C\left[\sin\left(\beta_i x\right) + \frac{\sin\left(\beta_i L\right)}{\sinh\left(\beta_i L\right)}\sinh\left(\beta_i x\right)\right]$$

In addition, the Eigenfunctions ψ_i utilized in the assumed mode method are orthogonal to each other, and therefore the following simplifications can be effected on the matrices

$$\hat{M}_{\alpha_{ij}} = \hat{M}_{\alpha_{ij}} = \begin{cases} 0 & (i \neq j) \\ \rho A L + \dfrac{1}{2} M_p \psi_i^2(p) & (i = j) \end{cases}$$

$$\hat{K}_{\alpha_{ij}} = \begin{cases} -k_{11}\psi_i(l)\psi_j(l) + k_p \psi_i(p)\psi_j(p) & (i \neq j) \\ EI\lambda_i^4 L + k_{11}\psi_i(l)\psi_j(l) + \psi_i(p)\psi_j(p) & (i = j) \end{cases}$$

$$\hat{K}_{\alpha_{ij}} = \begin{cases} -k_{21}\psi_i(l)\psi_j(l) + k_p \psi_i(p)\psi_j(p) & (i \neq j) \\ EI\lambda_i^4 L + k_{21}\psi_i(l)\psi_j(l) + \psi_i(p)\psi_j(p) & (i = j) \end{cases}$$

IV. NUMERICAL EXPERIMENTS

A. METHODOLOGY

Now that we have developed a mathematical model suitable for structural coupling of the trolley/RRDF interface, we need to develop some guidelines with regards to its applicability. One main question that we need to answer is whether such a model is indeed necessary for this problem. In order to assess this we proceed as follows:

1. First we evaluate the motions of the trolley/RRDF assuming that there is no structural coupling. This is achieved in the frequency domain utilizing results obtained by WAMIT. WAMIT is a software package that solves the hydrodynamic radiation/diffraction problem by a panel discretization of the body. It is a 3-dimensional program and as such it can model hydrodynamic interactions between multiple bodies. In our case the two bodies are the ship and the RRDF. Since we allow for hydrodynamic interactions (in other words the motion of each body depends on velocities and accelerations of the adjacent body) the equations of motion possess 12 degrees of freedom. Six degrees of freedom (surge, sway, yaw, heave, roll, pitch) come from each body.

2. Based on the computed body motions, we evaluate the relative motions at the interface between the two bodies; i.e., at the trolley end-points. These relative motions are subtracted (taking into consideration their relative phase angle) in order to obtain the angular displacement of the trolley as well as its twist.

3. The next step is to model the structural rigidity of the trolley through a generalized stiffness term. The relative motions of the trolley are then used to generate the reaction force in the trolley due to its stiffness. This force is then added to the hydrodynamic excitation force for the RRDF and the process continues. It should be mentioned that such coupling procedure is not necessary for the ship since, due to its high displacement, it is unlikely that it will be appreciably affected.

B.   RESULTS

Results are presented in the next chapter. All results are presented in standard polar plots in terms of the RMS value of the indicated response (trolley angle or twist). The radial coordinate of the graphs is the significant wave height, while the angular coordinate is the wave heading. Fully developed Pierson-Moskowitz and developing or decaying Bretchneider wave spectra are used for the calculations. Although the results have been obtained for long-crested seas, it is expected that the main conclusions will be valid for short-crested seas as well. The trolley stiffness that was introduced in the previous section is applied towards the roll motion of the RRDF. This is typical for a stern configuration. Similar results will apply for other trolley placements as well. For the numerical results that follow, the roll stiffness for the trolley has been normalized with respect to the roll stiffness of the RRDF. Naturally, the latter is a function of the RRDF displacement and its metacentric height.

V. RESULTS

A. TROLLEY ANGLE AND TWIST SUBJECTED TO PIERSON-MOSKOWITZ WAVE SPECTRUM

Figure (5) to (10) shows the RMS value of the trolley angle and trolley twist when subjected to the fully developed Pierson-Moskowitz wave spectrum for the cases where the normalized trolley stiffness was set to a value of 0, 1 and 2. 180 degrees corresponds to head seas while 0 degrees corresponds to following seas. The anti-symmetry in the fore and aft responds is due to the placement of the trolley on the aft of the ship. The slight anti-symmetry in the Port and Starboard responds is a result of the slight anti-symmetry of the shape of the RRDF. It is observed that the trolley angle is not being affected by the existence of the trolley stiffness or even if the trolley stiffness is doubled in strength. On the other hand, it is observed that the twist experienced by the trolley is significantly affected by the introduction of the trolley stiffness coupling term. The effect on the trolley twist is amplified further when the normalized trolley stiffness is doubled.

Figure 5.   RMS Value of Trolley Angle (degrees) subject to Pierce-Moskowitz spectrum and zero Roll stiffness

21

Figure 6.   RMS Value of Trolley Angle (degrees) subject to Pierce-Moskowitz spectrum and a Normalized Roll stiffness of 1

Figure 7.   RMS Value of Trolley Angle (degrees) subject to Pierce-Moskowitz spectrum and a Normalized Roll stiffness of 2
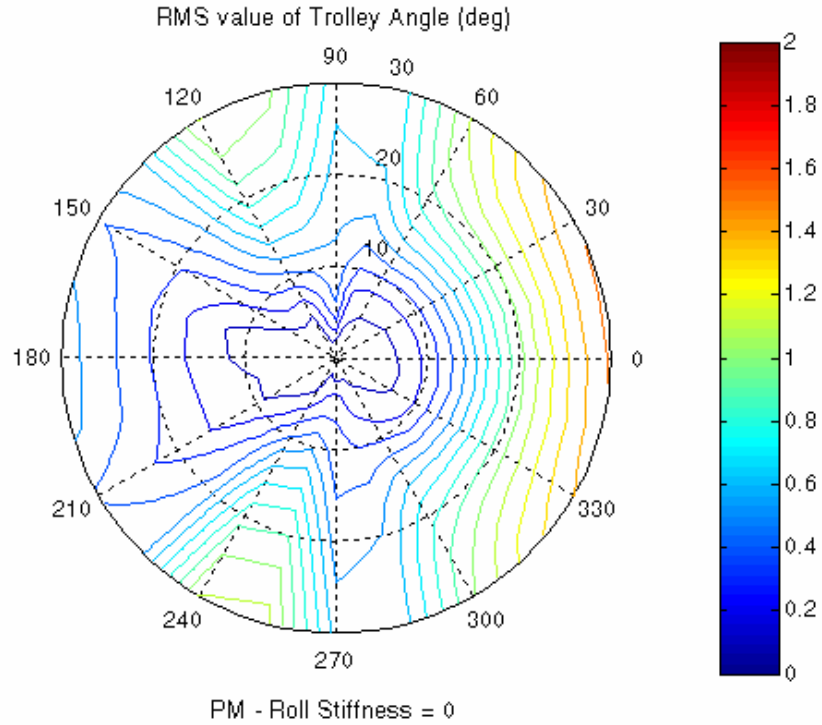
Figure 8.   RMS Value of Trolley Twist Angle (degrees) subject to Pierce-Moskowitz spectrum and zero Roll stiffness

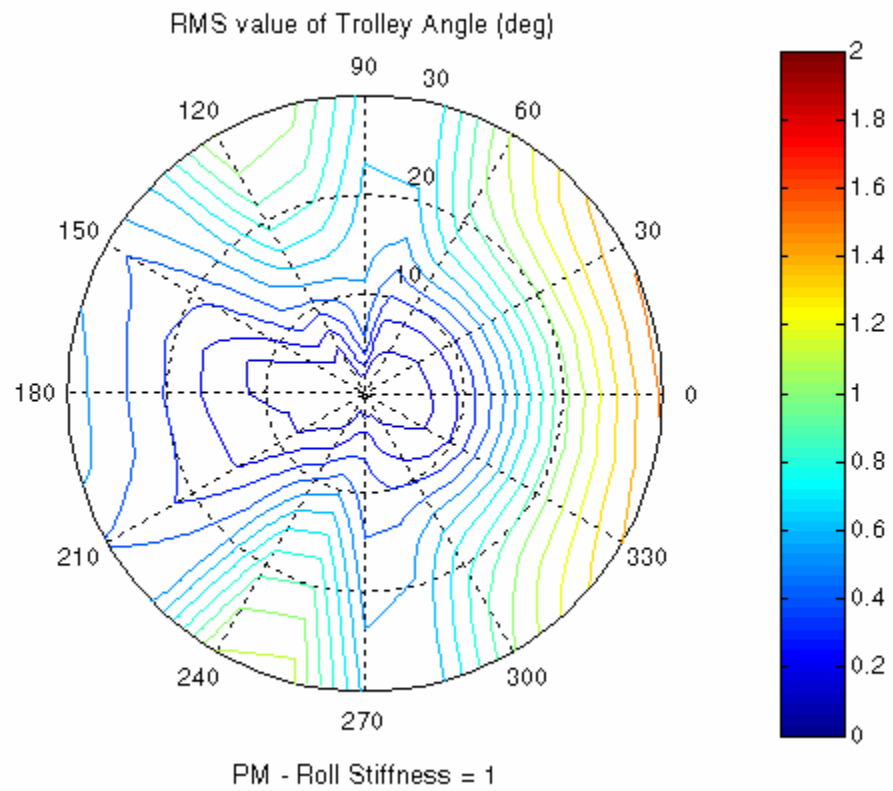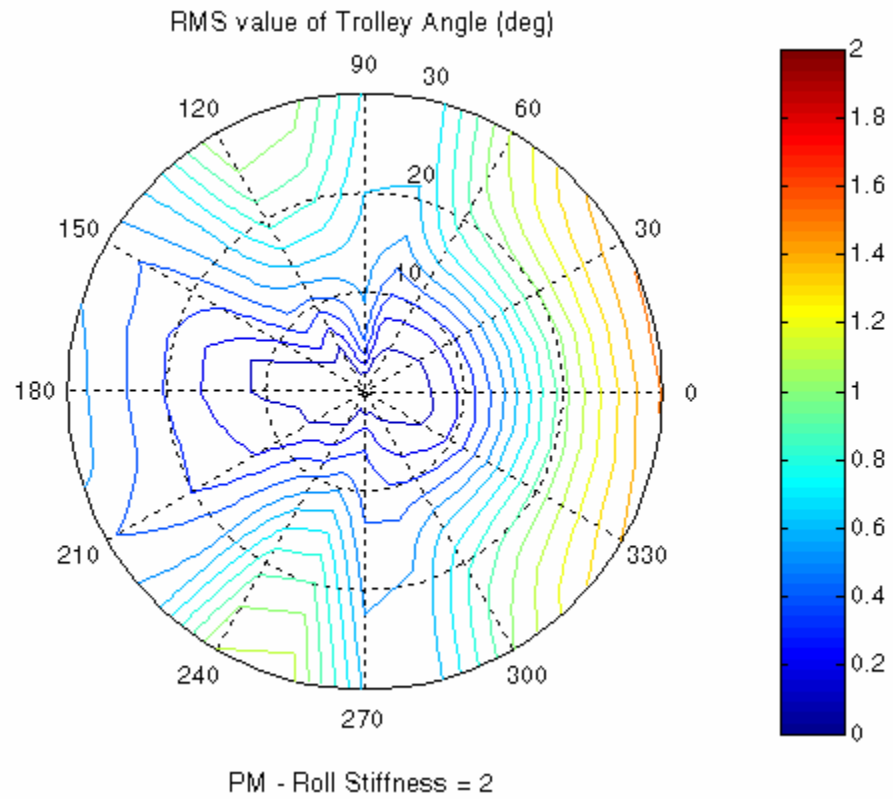RMS value of Trolley Twist (deg)

PM - Roll Stiffness = 1

Figure 9.   RMS Value of Trolley Twist Angle (degrees) subject to Pierce-Moskowitz spectrum and a Normalized Roll stiffness of 1
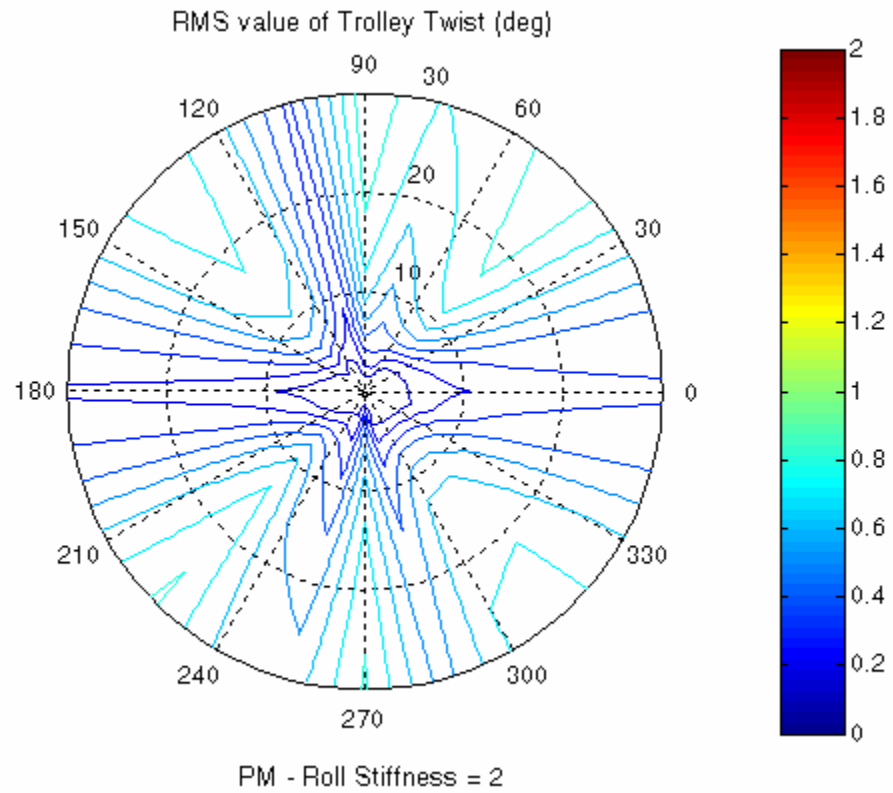
Figure 10.   RMS Value of Trolley Twist Angle (degrees) subject to Pierce-Moskowitz spectrum and a Normalized Roll stiffness of 2
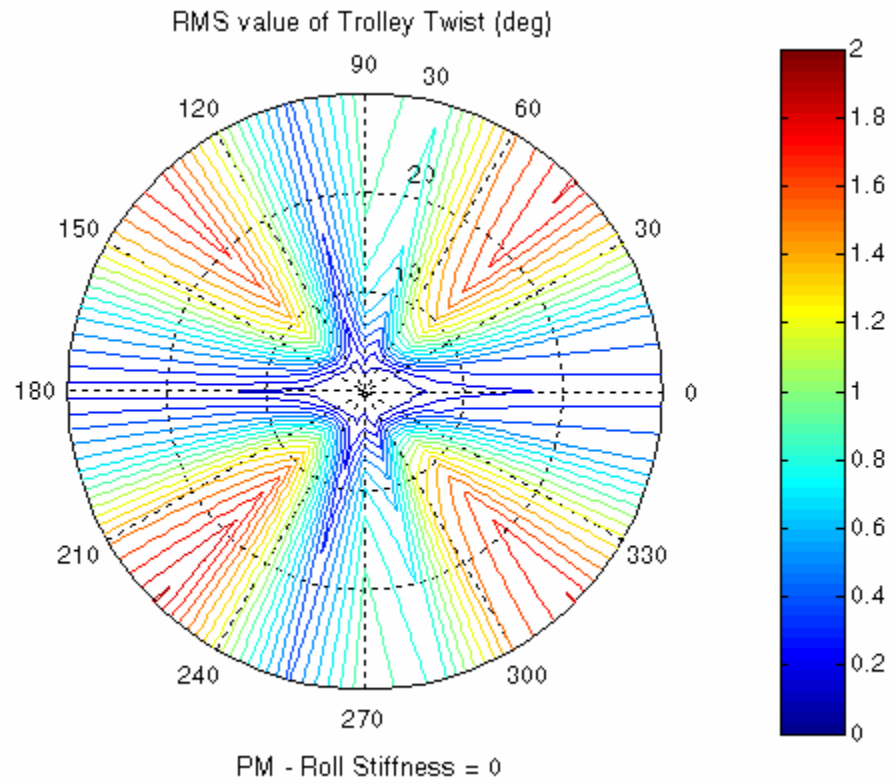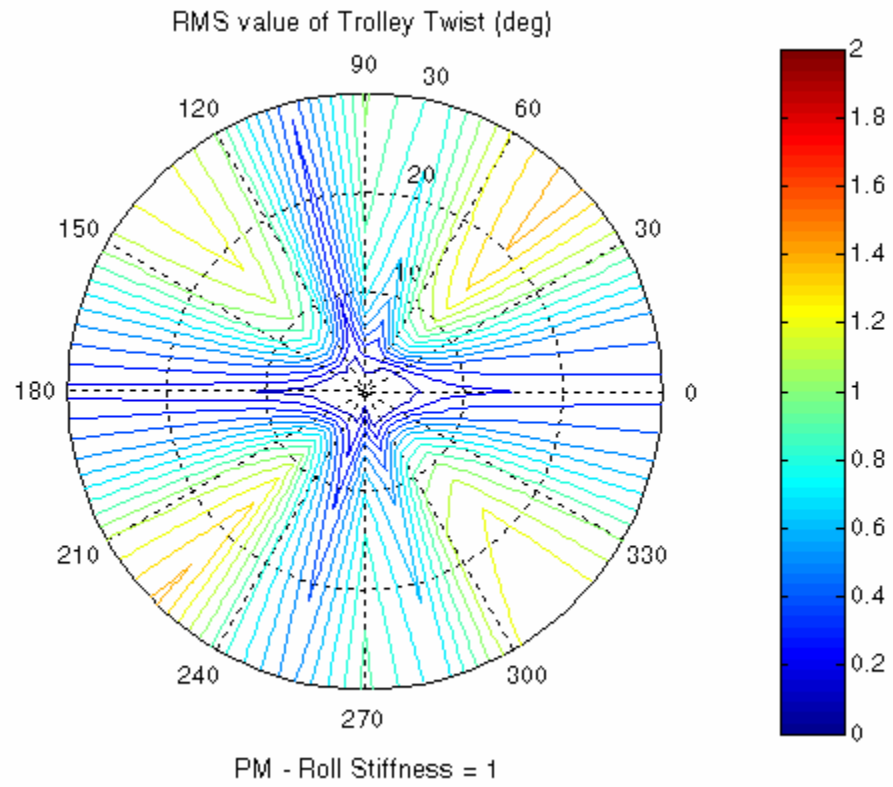
B. TROLLEY ANGLE AND TWIST SUBJECTED TO BRETSCHNEIDER WAVE SPECTRUM

Figure (11) to (22) shows the RMS value of the trolley angle and trolley twist when subjected to the Bretchneider wave spectrum for wave periods of 6 seconds and 12 seconds. The results are also presented for the three cases where the normalized trolley stiffness is set to a value of 0, 1 and 2. In this instance, we observe a similar trend in the results with the case under the Pierson-Moskowitz wave spectrum – the trolley angle does not seems to be affected by the existence of the trolley stiffness coupling term while the trolley twist is substantially affected by the introduction of the trolley stiffness and the effects are amplified with an increased in the strength of the coupling term.

Figure 11.   RMS Value of Trolley Angle (degrees) subject to Bretchneider spectrum with a wave period of 6 seconds and zero Roll stiffness

27

Figure 12.   RMS Value of Trolley Angle (degrees) subject to Bretchneider spectrum with a
wave period of 6 seconds and a Normalized Roll stiffness of 1

Figure 13.   RMS Value of Trolley Angle (degrees) subject to Bretchneider spectrum with a wave period of 6 seconds and a Normalized Roll stiffness of 2
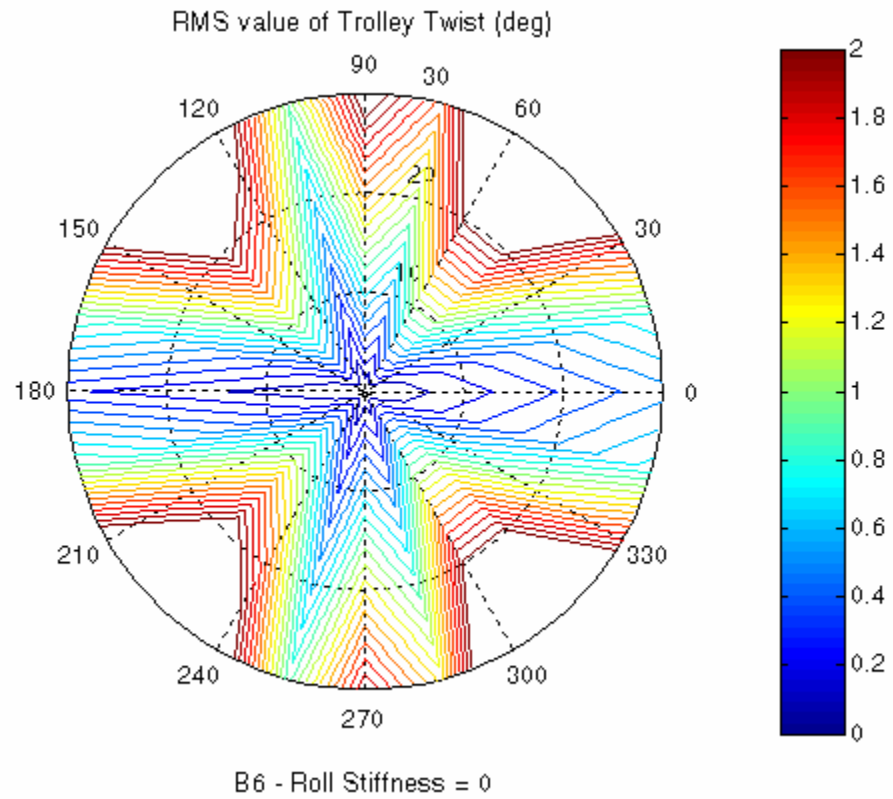
Figure 14.   RMS Value of Trolley Twist Angle (degrees) subject to Bretchneider spectrum with a wave period of 6 seconds and zero Roll stiffness
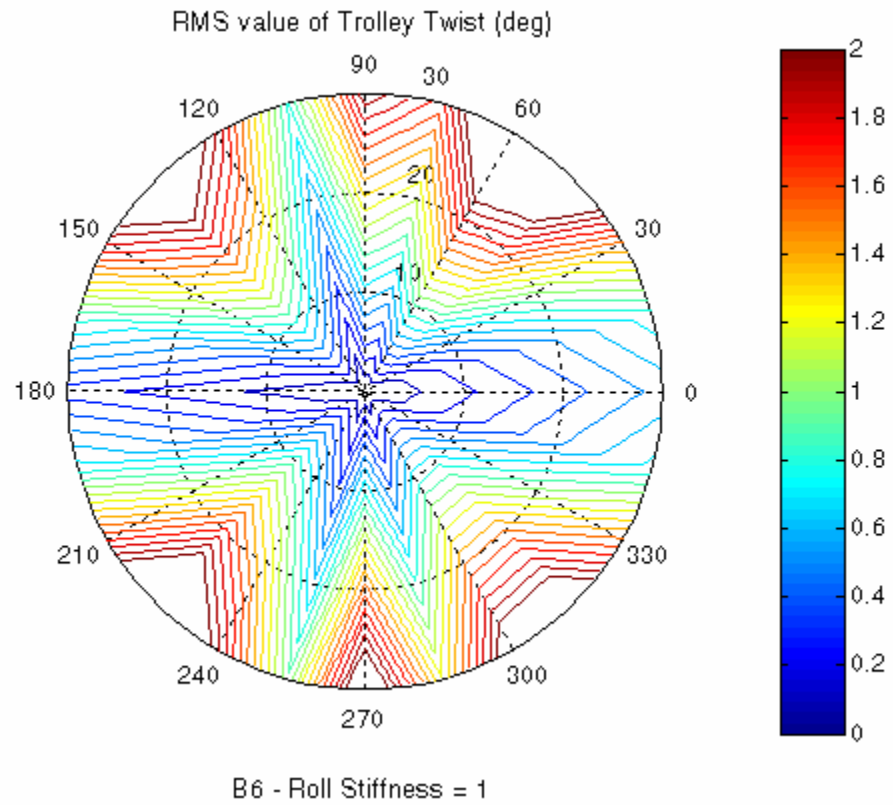
Figure 15.   RMS Value of Trolley Twist Angle (degrees) subject to Bretchneider spectrum with a wave period of 6 seconds and a Normalized Roll stiffness of 1
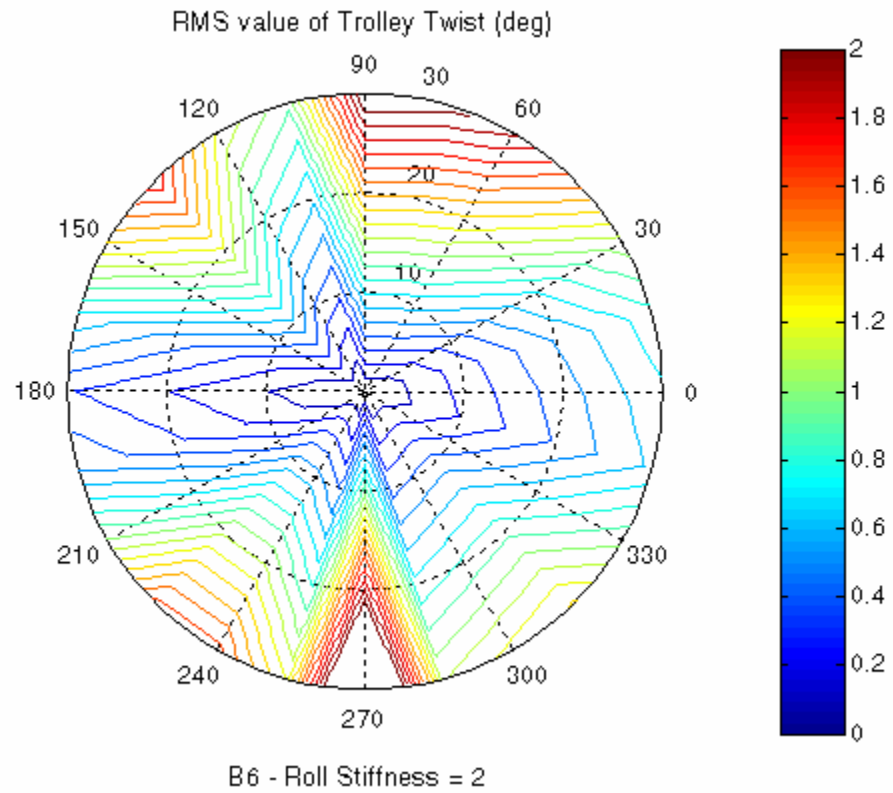
Figure 16.   RMS Value of Trolley Twist Angle (degrees) subject to Bretchneider spectrum with a wave period of 6 seconds and a Normalized Roll stiffness of 2
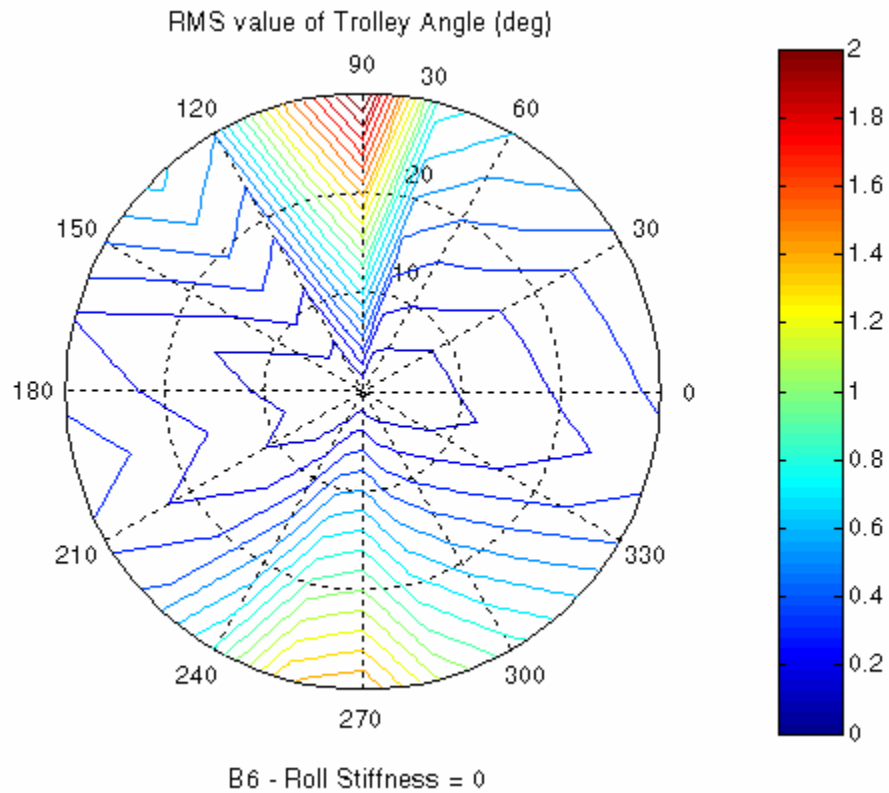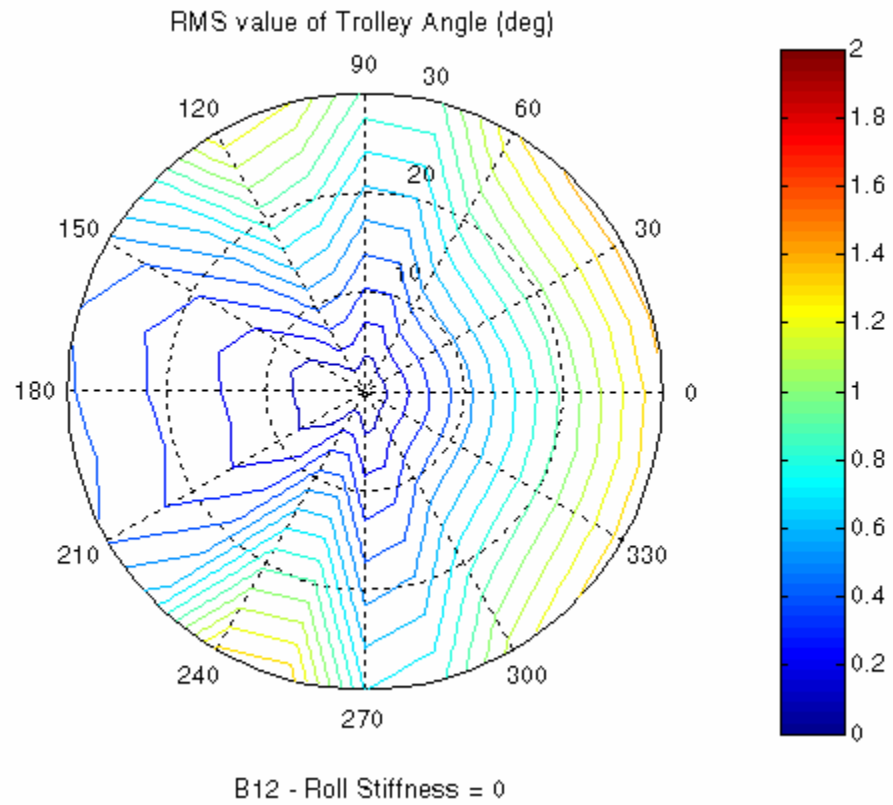
Figure 17.　RMS Value of Trolley Angle (degrees) subject to Bretchneider spectrum with a wave period of 12 seconds and zero Roll stiffness
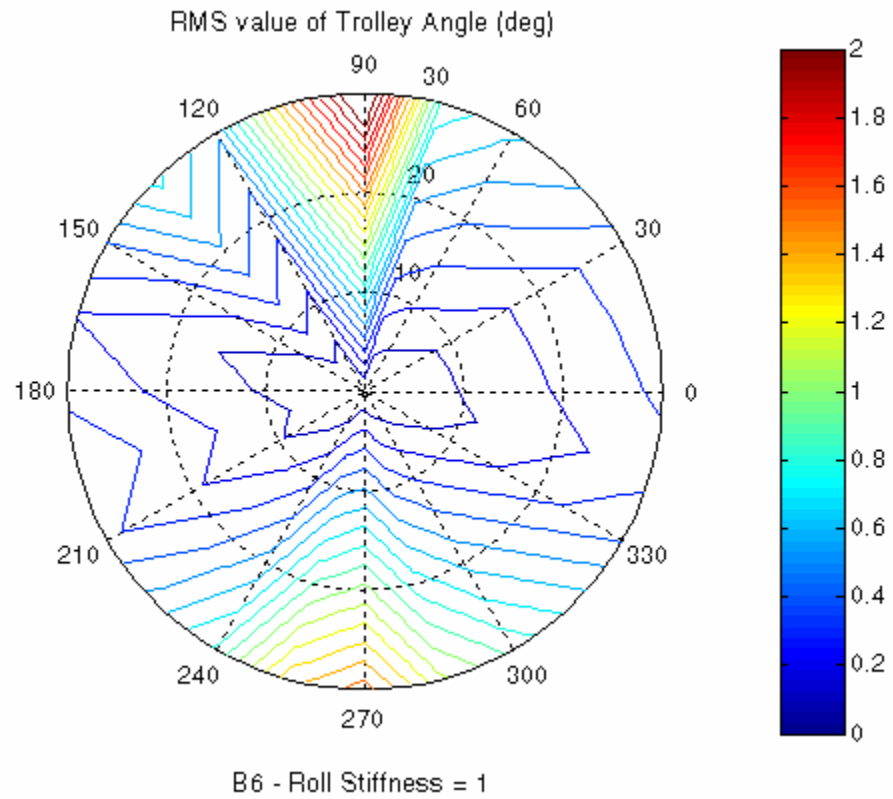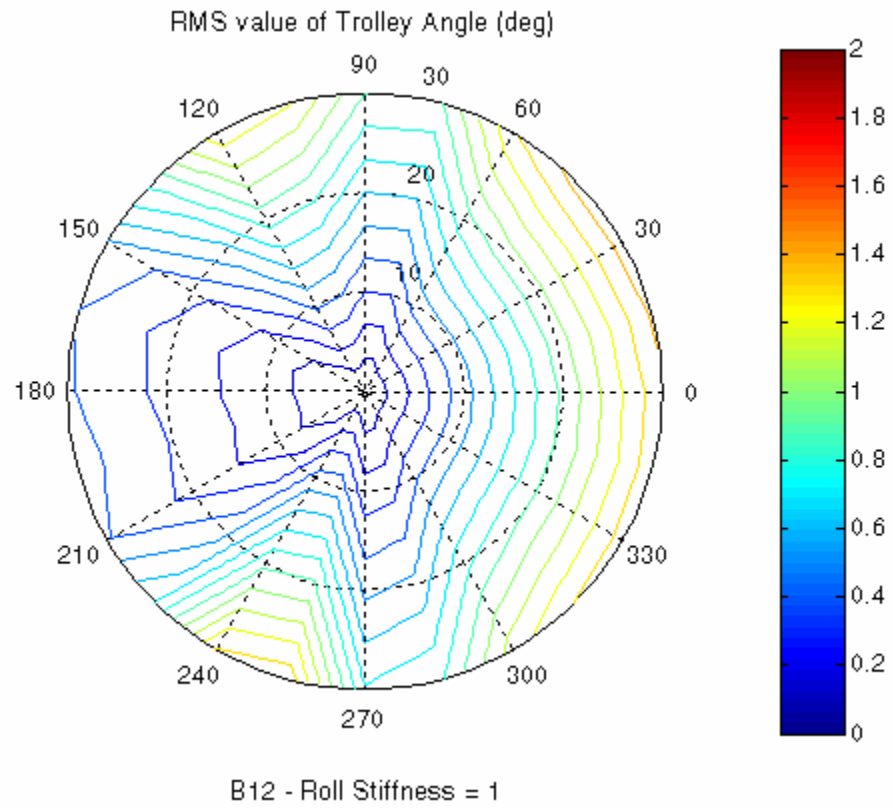
Figure 18.   RMS Value of Trolley Angle (degrees) subject to Bretchneider spectrum with a wave period of 12 seconds and a Normalized Roll stiffness of 1
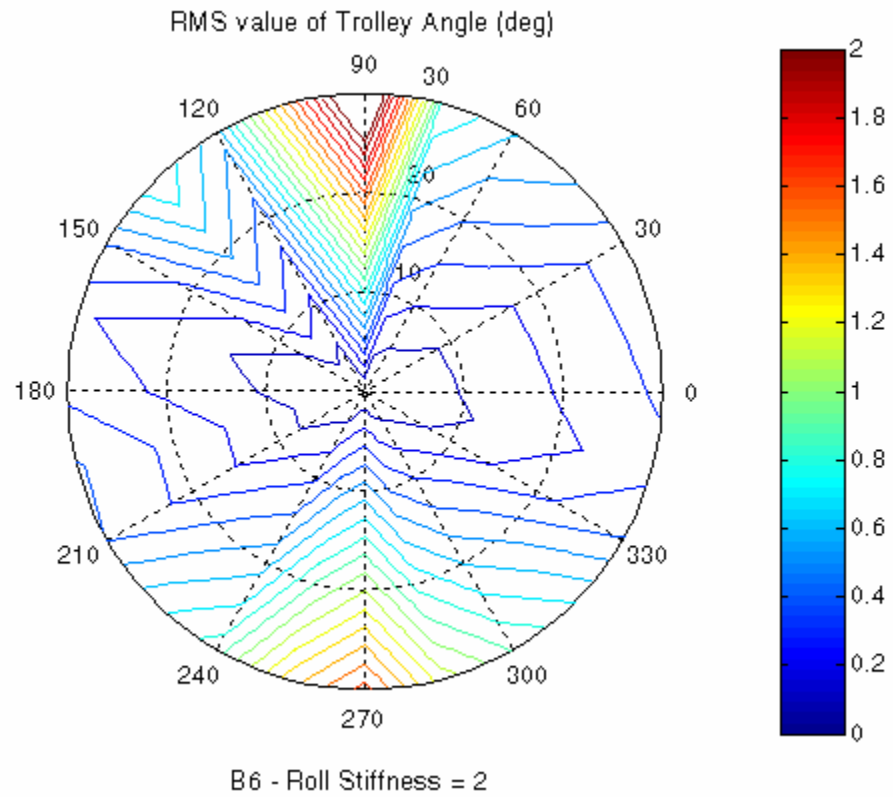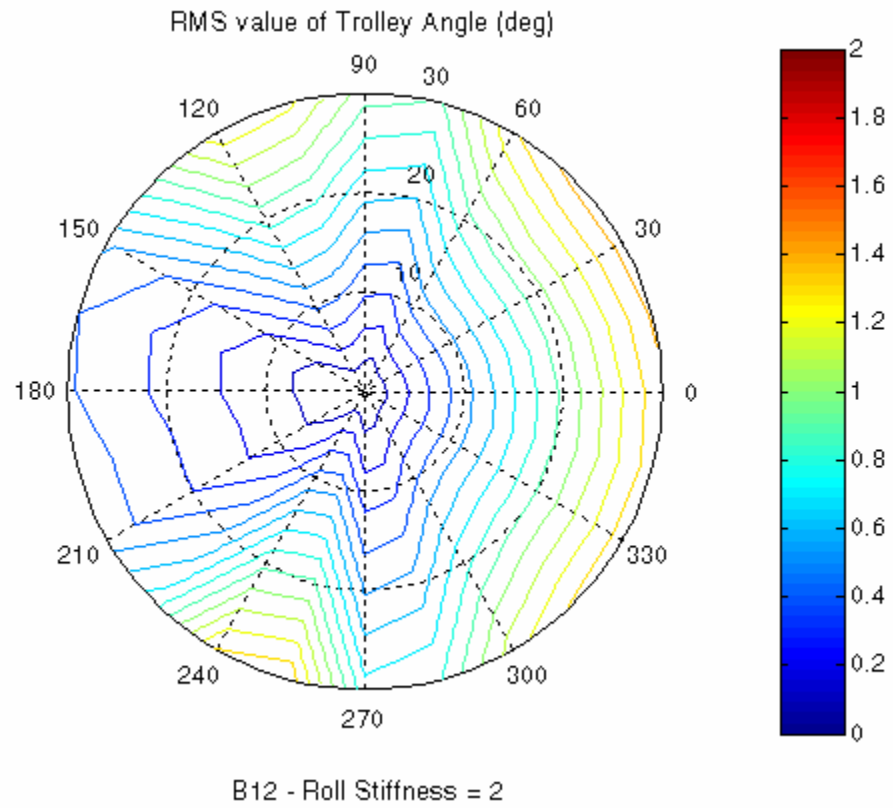
Figure 19.   RMS Value of Trolley Angle (degrees) subject to Bretchneider spectrum with a wave period of 12 seconds and a Normalized Roll stiffness of 2
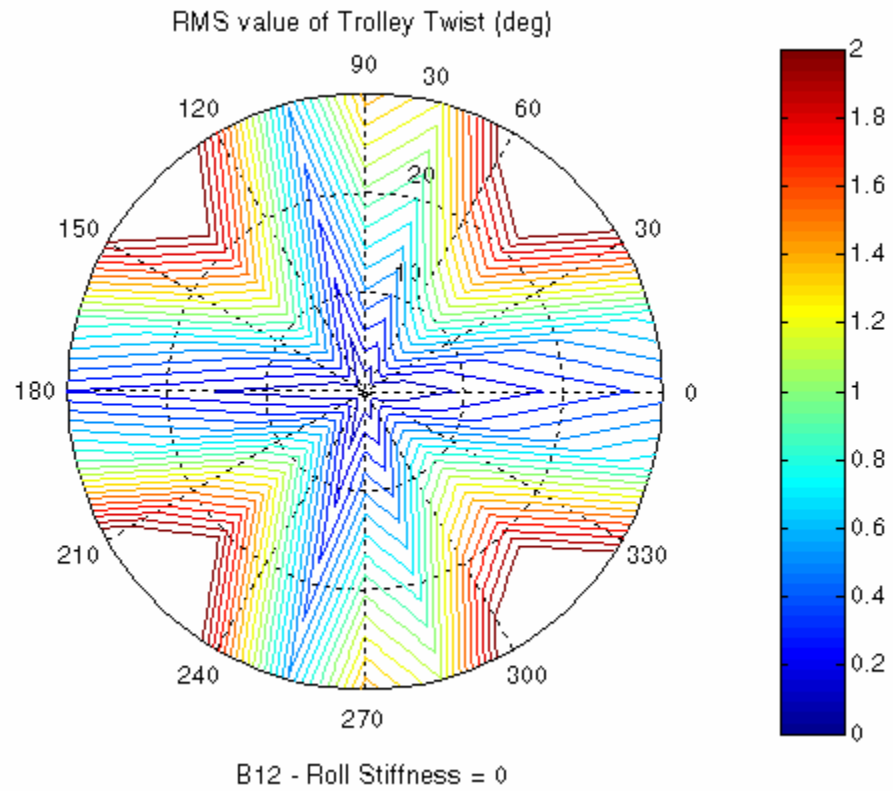
Figure 20.   RMS Value of Trolley Twist Angle (degrees) subject to Bretchneider spectrum
with a wave period of 12 seconds and zero Roll stiffness
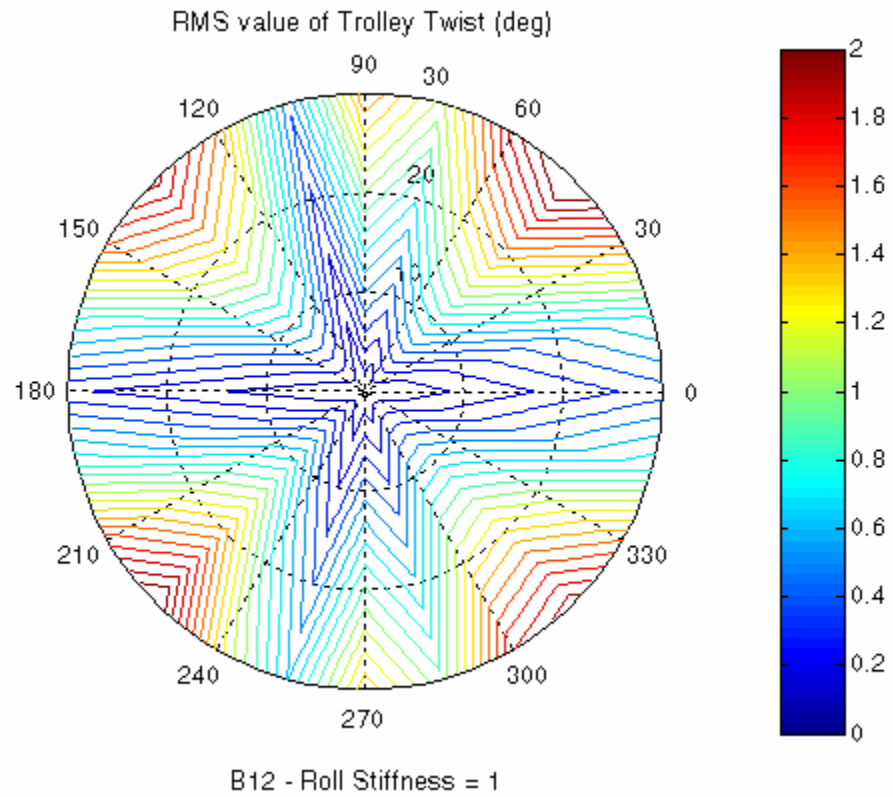
Figure 21.   RMS Value of Trolley Twist Angle (degrees) subject to Bretchneider spectrum
with a wave period of 12 seconds and a Normalized Roll stiffness of 1
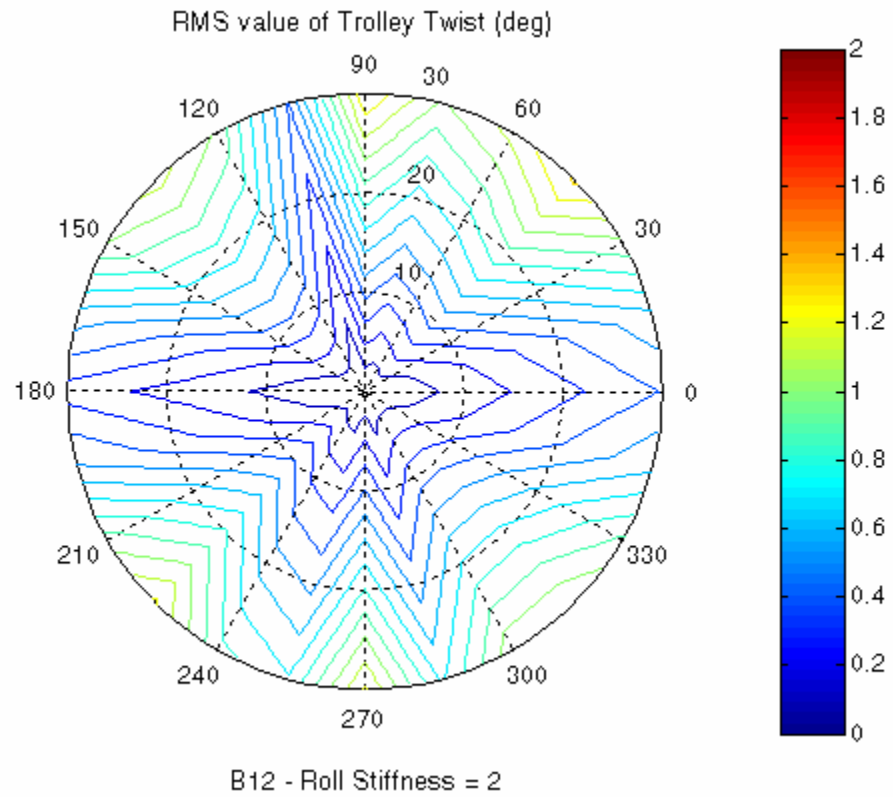
Figure 22.   RMS Value of Trolley Twist Angle (degrees) subject to Bretchneider spectrum with a wave period of 12 seconds and a Normalized Roll stiffness of 2

C.   INFLUENCE OF TROLLEY STIFFNESS ON TROLLEY TWIST

The observations from the previous sections are better illustrated through Figure (23) to (28), which shows the comparison of the responds of the trolley angle and trolley twist, with and without the trolley stiffness coupling term.   The almost symmetrical response of Port and Starboard direction is expected with the slight variation being accounted for by the slight anti-symmetry of the shape of the RRDF.   It can clearly be seen that there is substantial differences in the responds of the trolley twist when the stiffness coupling term is introduced.   This responds is magnified when the coupling term is doubled.   In addition, it is observed that the quartering seas results in higher trolley twist.
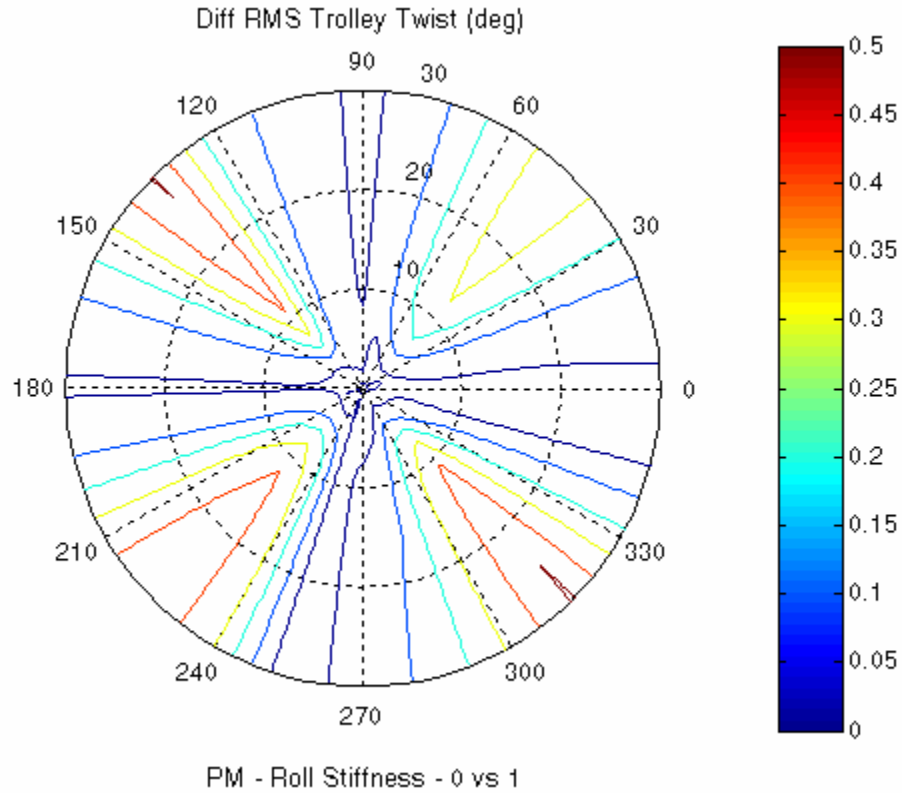
Figure 23.   Difference in average vertical trolley twist angle for a Normalized Roll stiffness of 0 and 1 (subjected to Pierce-Moskowitz wave spectrum)
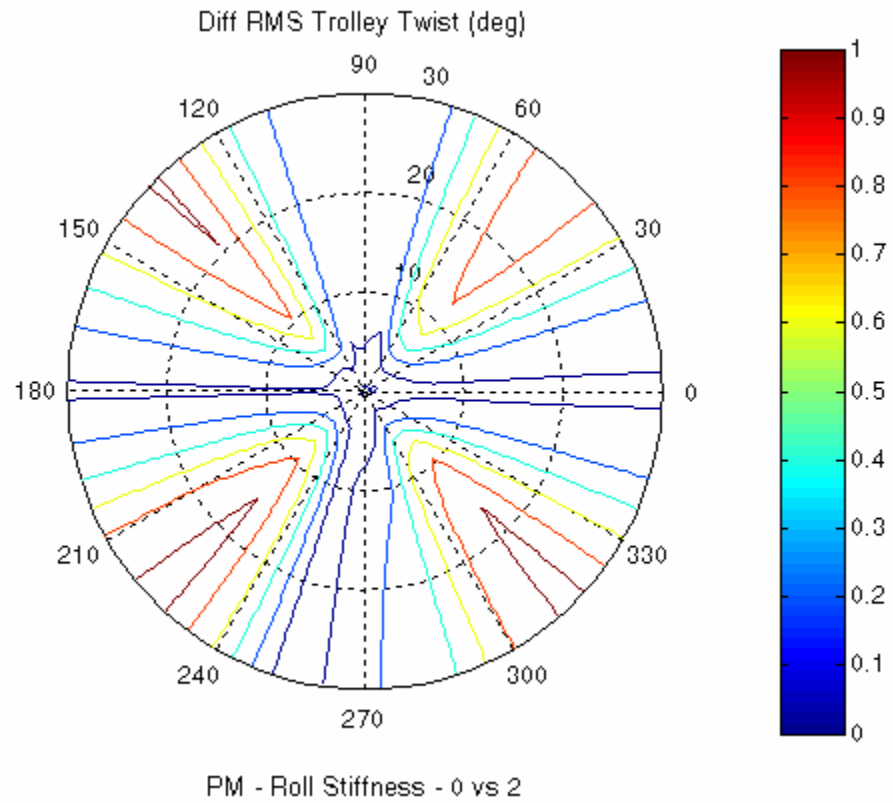
Figure 24.   Difference in average vertical trolley twist angle for a Normalized Roll stiffness of 0 and 2 (subjected to Pierce-Moskowitz wave spectrum)

Diff RMS Trolley Twist (deg)

B6 - Roll Stiffness - 0 vs 1
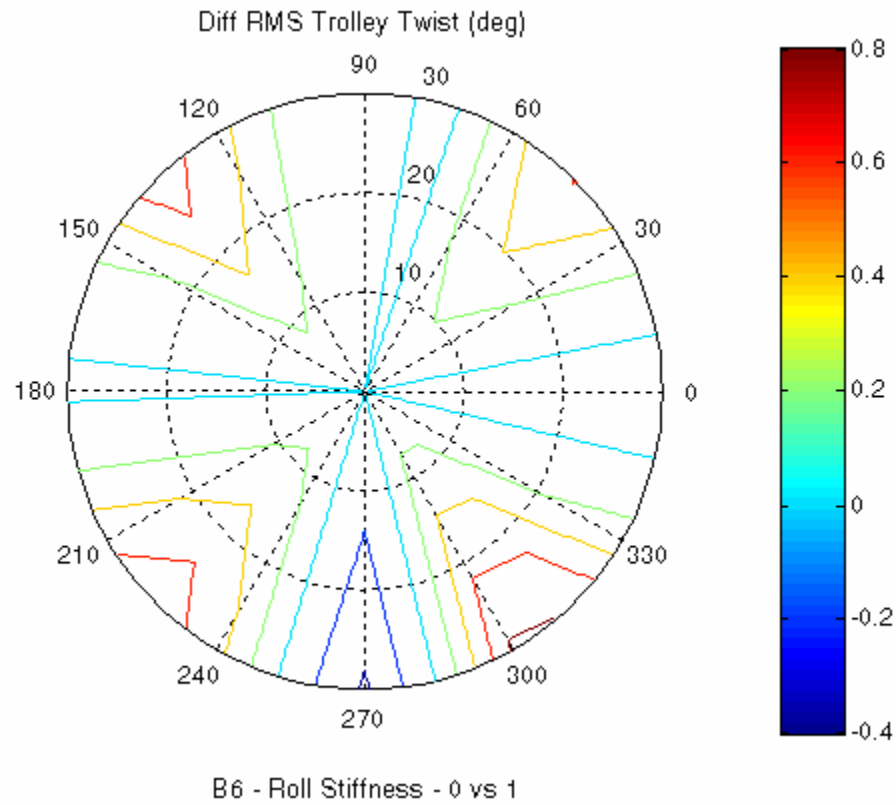
Figure 25.   Difference in average vertical trolley twist angle for a Normalized Roll stiffness of 0 and 1 (subjected to Bretchneider spectrum with a wave period of 6 seconds)

Diff RMS Trolley Twist (deg)

B 6 - Roll Stiffness - 0 vs 2
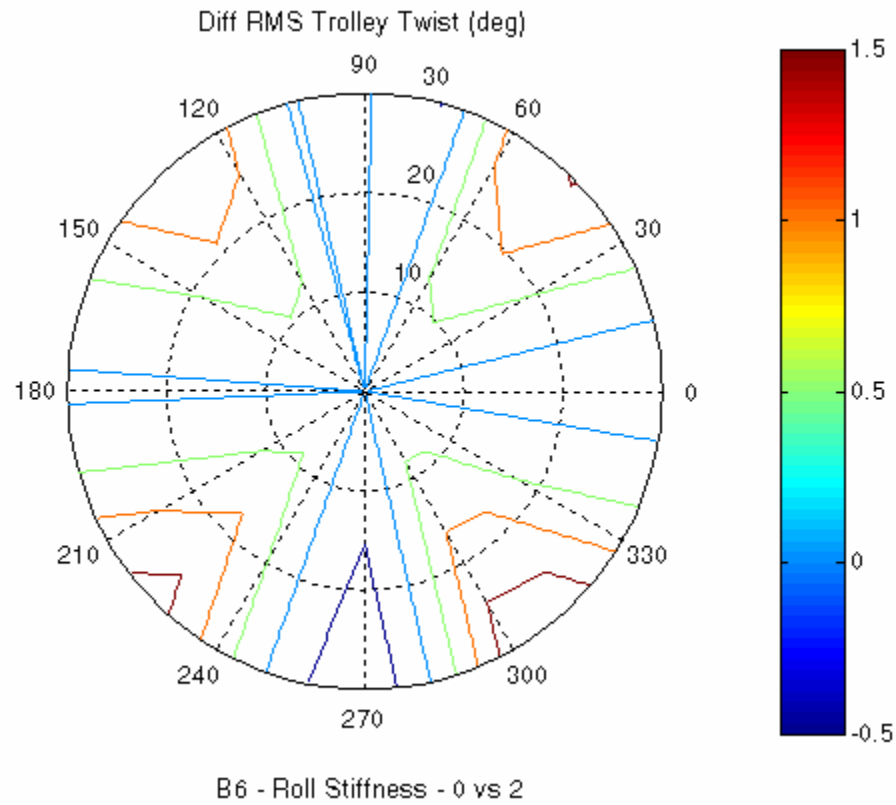
Figure 26.   Difference in average vertical trolley twist angle for a Normalized Roll stiffness
of 0 and 2 (subjected to Bretchneider spectrum with a wave period of 6 seconds)
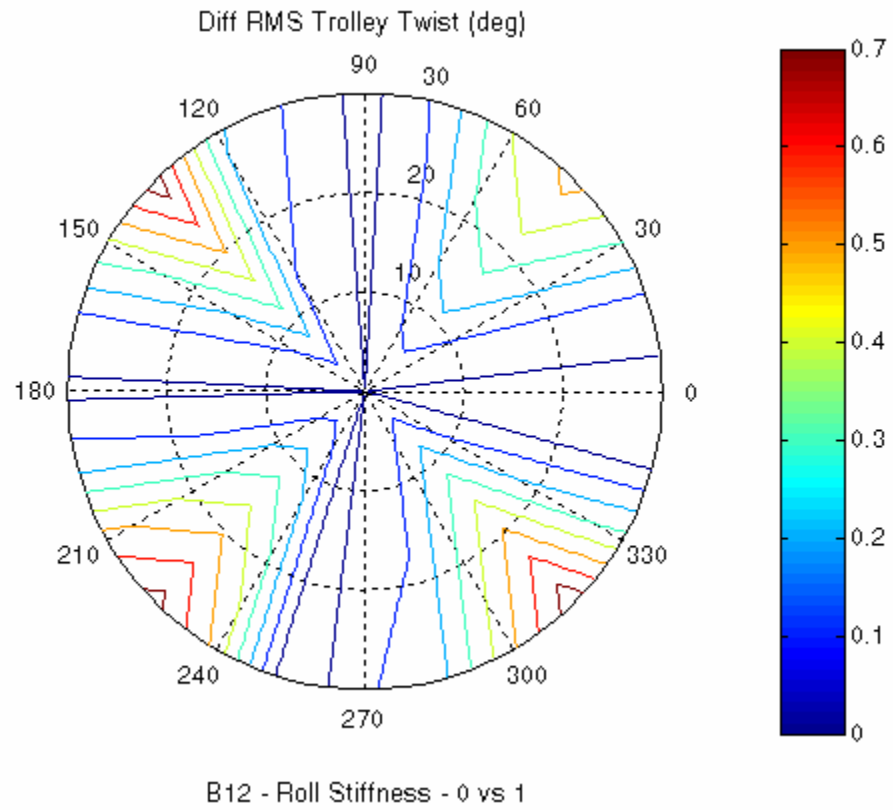
Figure 27.   Difference in average vertical trolley twist angle for a Normalized Roll stiffness of 0 and 1 (subjected to Bretchneider spectrum with a wave period of 12 seconds)
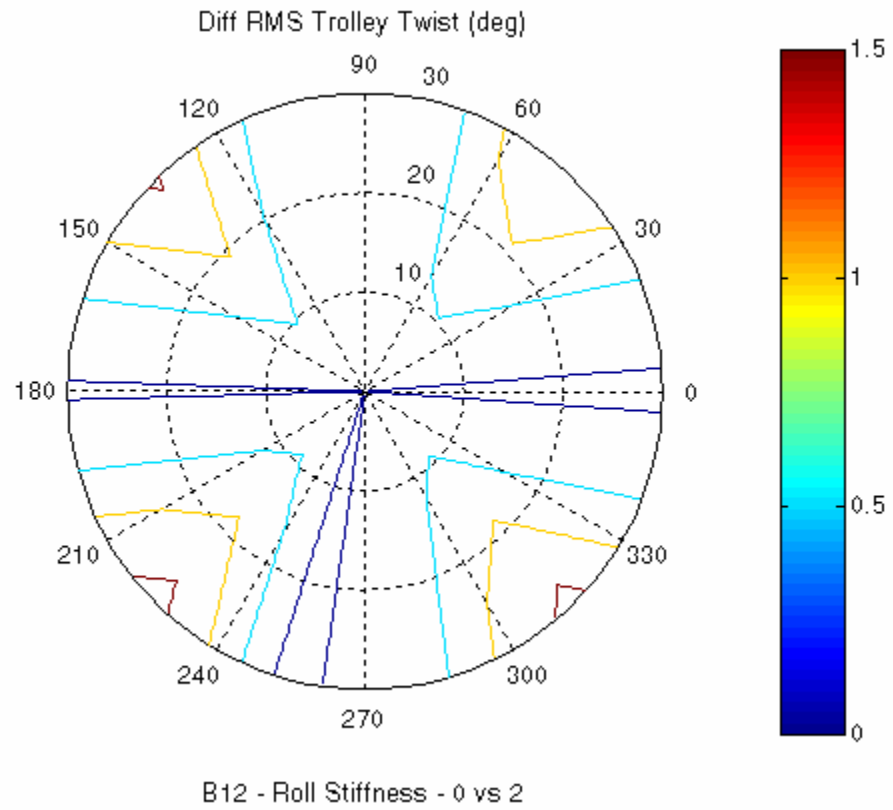
Figure 28. Difference in average vertical trolley twist angle for a Normalized Roll stiffness of 0 and 2 (subjected to Bretchneider spectrum with a wave period of 12 seconds)

VI. CONCLUSIONS AND RECOMMENDATIONS

A. CONCLUSIONS

This thesis has laid the foundation for the analyzing of structural coupling effects for the proposed trolley interface between a ship and a Roll-on Roll-off Discharge Facility (RRDF) through the development of a mathematical model utilizing Assumed Modes and Virtual Work techniques, which incorporates the structural coupling effects of the trolley to the RRDF. Through a systematic series of numerical experiments, it was also determined that the trolley angle is not affected by the structural coupling effects, in contrast with the trolley twist which is substantially affected by structural coupling.

B. RECOMMENDATIONS FOR FUTURE WORK

1. Side Trolley Placement

We have conducted the analysis for stern placement of the new trolley-rail system. However there are cases where the trolley-rail system may be placed on the side of the ship for unloading operations. In this scenario, the hydrodynamic coupling effects of the ship and the RRDF will be significantly different. A similar analysis should be conducted for the side trolley placement to determine the relative impact of the structural coupling effects.

2. Structural Coupling for Trolley Twist

Given the knowledge that the trolley twist is substantially affected by structural coupling between the trolley and RRDF, we can now proceed to analyze the structural coupling effects utilizing the mathematical model developed, so that appropriate measures can be taken to ensure that cargo transfer can be conducted at sea up to Sea state 5.

THIS PAGE INTENTIONALLY LEFT BLANK

APPENDIX A

MATLAB CODE

```
% Motions calculation for CapeD/RRDF/trolley interface.
% Long-crested Bretchneider seas.
%
i_seaway=input('Enter 0 for PM or 1 for Bretchneider spectrum = ');
if i_seaway == 1
    T_m =input('Modal Period (sec) = ');
    omega_m=2*pi/T_m;
end
i_stiffness=input('Enter 3 for heave stiffness, 4 for roll, or 5 for pitch = ');
k_stiffness=input('Enter appropriate normalized stiffness = ');
%
x_arm_CAPED_1=-330;
x_arm_CAPED_2=-330;
y_arm_CAPED_1=-10;
y_arm_CAPED_2=+10;
x_arm_RRDF_1=20;
x_arm_RRDF_2=20;
y_arm_RRDF_1=-10;
y_arm_RRDF_2=+10;
trolley_length=100;
%
% Load processed WAMIT data file
%
load CAPED
NH=25;
i_NH=15;
beta_incr=i_NH;
imag_unit=sqrt(-1);
%
```

```
% Set the frequencies vector (0.3 to 2.5 rad/sec)
%
NF=(size(frequencies));
NF=NF(1,1);
w=frequencies;
%
% Set the headings vector (0 to 360 degrees in i_NH deg. increments)
%
for i=1:NH,
    heading(i)=i_NH*(i-1);
end
%
% Set added mass and damping matrices and forcing vector
%
for i=1:NF,
    i_string=num2str(i);
    A(:,:,i)=eval(strcat('admassfreq',i_string));
    B(:,:,i)=eval(strcat('addumpingfreq',i_string));
    for j=1:NH,
        j_string=num2str(j);
        if j==NH
            j_string=num2str(1);
        end
        F(:,i,j)=eval(strcat('forcfreq',i_string,'head',j_string));
    end
end
%
% Random wave calculations
% PM spectrum - weighted by the spreading function
%
% Loop on significant wave height
iHS=0;
for HS=0.5:0.5:30,
```

```
HS;
iHS=iHS+1;
if i_seaway ==0
    omega_m=0.4*sqrt(32.2/HS);
end
A_s=(1.25/4)*(omega_m^4)*(HS^2);
B_s=1.25*omega_m^4;
S_main=(A_s./w.^5).*exp(-B_s./w.^4);
%
% Loop on sea direction
%
ibeta=0;
for beta=0:beta_incr:360,
    beta_set=beta;
    ibeta=ibeta+1;
    S=S_main;
    heading_single=heading(ibeta);
    %
    % Frequency domain response is given by x= [-w^2*(A+mass)+i*w*B+C]^(-1)*F
    % Zeroth order calculation (no trolley/RRDF structural coupling)
    %
    for i=1:NF,
        w_single=w(i);
        A_bar=-w_single*w_single*(A(:,:,i))+imag_unit*w_single*B(:,:,i)+C;
        F_bar=F(:,i,ibeta);
        x=inv(A_bar)*F_bar;
        %
        % Ship motions
        %
        surge0_CAPED(i) = x(1);
        sway0_CAPED(i) = x(2);
        heave0_CAPED(i)  = x(3);
        roll0_CAPED(i)  = x(4);
```
49

```matlab
        pitch0_CAPED(i) = x(5);
        yaw0_CAPED(i)   = x(6);
        %
        % RRDF motions
        %
        surge0_RRDF(i) = x(7);
        sway0_RRDF(i) = x(8);
        heave0_RRDF(i)  = x(9);
        roll0_RRDF(i)  = x(10);
        pitch0_RRDF(i) = x(11);
        yaw0_RRDF(i)   = x(12);
        %
        % Motions/ at trolley end - CAPED side
        %
        m0_t_CAPED_v_1(i)=heave0_CAPED(i)-
x_arm_CAPED_1*pitch0_CAPED(i)...
            -y_arm_CAPED_1*roll0_CAPED(i);
        m0_t_CAPED_v_2(i)=heave0_CAPED(i)-
x_arm_CAPED_2*pitch0_CAPED(i)...
            -y_arm_CAPED_2*roll0_CAPED(i);

m0_t_CAPED_h_1(i)=abs(sway0_CAPED(i))+x_arm_CAPED_1*abs(yaw0_CAPED(i))
;

m0_t_CAPED_h_2(i)=abs(sway0_CAPED(i))+x_arm_CAPED_2*abs(yaw0_CAPED(i))
;
        %
        % Motions at trolley end - RRDF side
        %
        m0_t_RRDF_v_1(i)=heave0_RRDF(i)-x_arm_RRDF_1*pitch0_RRDF(i)...
          -y_arm_RRDF_1*roll0_RRDF(i);
        m0_t_RRDF_v_2(i)=heave0_RRDF(i)-x_arm_RRDF_2*pitch0_RRDF(i)...
          -y_arm_RRDF_2*roll0_RRDF(i);

m0_t_RRDF_h_1(i)=abs(sway0_RRDF(i))+x_arm_RRDF_1*abs(yaw0_RRDF(i));
```

```
m0_t_RRDF_h_2(i)=abs(sway0_RRDF(i))+x_arm_RRDF_2*abs(yaw0_RRDF(i));
    %
    % Trolley relative vertical angular displacement
    %
    m0_trolley_angle_v_1(i)=(abs(heave0_CAPED(i))-
x_arm_CAPED_1*abs(pitch0_CAPED(i))...
        -y_arm_CAPED_1*abs(roll0_CAPED(i))-(abs(heave0_RRDF(i))-
x_arm_RRDF_1*abs(pitch0_RRDF(i))...
        -y_arm_RRDF_1*abs(roll0_RRDF(i))))/trolley_length;
    m0_trolley_angle_v_2(i)=(abs(heave0_CAPED(i))-
x_arm_CAPED_2*abs(pitch0_CAPED(i))...
        -y_arm_CAPED_2*abs(roll0_CAPED(i))-(abs(heave0_RRDF(i))-
x_arm_RRDF_2*abs(pitch0_RRDF(i))...
        -y_arm_RRDF_2*abs(roll0_RRDF(i))))/trolley_length;
    %
    % Trolley relative horizontal displacement
    %
    m0_trolley_distance_h_1(i)=(m0_t_CAPED_h_1(i)-m0_t_RRDF_h_1(i));
    m0_trolley_distance_h_2(i)=(m0_t_CAPED_h_2(i)-m0_t_RRDF_h_2(i));
    %
    % Calculate transmission force due to trolley end-points motion differential
    %
    if i_stiffness==3
       f_diff(i)=C(9,9)*k_stiffness*(m0_t_RRDF_v_1(i)-m0_t_RRDF_v_2(i));
       heave_trolley(i)=f_diff(i);
       roll_trolley(i)=0;
       pitch_trolley(i)=0;
    end
    if i_stiffness==4
       f_diff(i)=C(10,10)*k_stiffness*abs((m0_trolley_angle_v_1(i)-
m0_trolley_angle_v_2(i)));
       heave_trolley(i)=0;
       roll_trolley(i)=f_diff(i);
```

```
        pitch_trolley(i)=0;
    end
    if i_stiffness==5
        f_diff(i)=C(11,11)*k_stiffness*abs((m0_trolley_angle_v_1(i)-
m0_trolley_angle_v_2(i)));
        heave_trolley(i)=0;
        roll_trolley(i)=0;
        pitch_trolley(i)=f_diff(i);
    end
end
%
% First-order correction
% Calculate motions again incorporating trolley stiffness correction
%
for i=1:NF,
    w_single=w(i);
    A_bar=-w_single*w_single*(A(:,:,i))+imag_unit*w_single*B(:,:,i)+C;
    f_trolley=f_diff(i);
    m_trolley=f_diff(i)*20;
    F_bar=F(:,i,ibeta)+[0;0;0;0;0;0;0;0;heave_trolley(i);-
roll_trolley(i);pitch_trolley(i);0];
    x=inv(A_bar)*F_bar;
    %
    % Ship motions
    %
    surge_CAPED(i) = x(1);
    sway_CAPED(i) = x(2);
    heave_CAPED(i)  = x(3);
    roll_CAPED(i)  = x(4);
    pitch_CAPED(i) = x(5);
    yaw_CAPED(i)   = x(6);
    %
    % RRDF motions
```

```
%
surge_RRDF(i) = x(7);
sway_RRDF(i) = x(8);
heave_RRDF(i)  = x(9);
roll_RRDF(i)  = x(10);
pitch_RRDF(i) = x(11);
yaw_RRDF(i)   = x(12);
%
% Motions/ at trolley end - CAPED side
%
m_t_CAPED_v_1(i)=heave_CAPED(i)-x_arm_CAPED_1*pitch_CAPED(i)...
   -y_arm_CAPED_1*roll_CAPED(i);
m_t_CAPED_v_2(i)=heave_CAPED(i)-x_arm_CAPED_2*pitch_CAPED(i)...
   -y_arm_CAPED_2*roll_CAPED(i);

m_t_CAPED_h_1(i)=abs(sway_CAPED(i))+x_arm_CAPED_1*abs(yaw_CAPED(i));

m_t_CAPED_h_2(i)=abs(sway_CAPED(i))+x_arm_CAPED_2*abs(yaw_CAPED(i));
%
% Motions at trolley end - RRDF side
%
m_t_RRDF_v_1(i)=heave_RRDF(i)-x_arm_RRDF_1*pitch_RRDF(i)...
   -y_arm_RRDF_1*roll_RRDF(i);
m_t_RRDF_v_2(i)=heave_RRDF(i)-x_arm_RRDF_2*pitch_RRDF(i)...
   -y_arm_RRDF_2*roll_RRDF(i);
m_t_RRDF_h_1(i)=abs(sway_RRDF(i))+x_arm_RRDF_1*abs(yaw_RRDF(i));
m_t_RRDF_h_2(i)=abs(sway_RRDF(i))+x_arm_RRDF_2*abs(yaw_RRDF(i));
%
% Trolley relative vertical angular displacement
%
m_trolley_angle_v_1(i)=(abs(heave_CAPED(i))-
x_arm_CAPED_1*abs(pitch_CAPED(i))...
      -y_arm_CAPED_1*abs(roll_CAPED(i))-(abs(heave_RRDF(i))-
x_arm_RRDF_1*abs(pitch_RRDF(i))...
```

```matlab
            -y_arm_RRDF_1*abs(roll_RRDF(i))))/trolley_length;
        m_trolley_angle_v_2(i)=(abs(heave_CAPED(i))-
x_arm_CAPED_2*abs(pitch_CAPED(i))...
            -y_arm_CAPED_2*abs(roll_CAPED(i))-(abs(heave_RRDF(i))-
x_arm_RRDF_2*abs(pitch_RRDF(i))...
            -y_arm_RRDF_2*abs(roll_RRDF(i))))/trolley_length;
        m_trolley_angle_v_twist(i)=m_trolley_angle_v_1(i)-m_trolley_angle_v_2(i);

m_trolley_angle_v_average(i)=0.5*(m_trolley_angle_v_1(i)+m_trolley_angle_v_2(i));
    %
    % Trolley relative horizontal displacement
    %
    m_trolley_distance_h_1(i)=(m_t_CAPED_h_1(i)-m_t_RRDF_h_1(i));
    m_trolley_distance_h_2(i)=(m_t_CAPED_h_2(i)-m_t_RRDF_h_2(i));
    end
%
% Define response spectra
%
S_surge_CAPED = ((abs(surge_CAPED)).^2).*S';
S_surge_RRDF  = ((abs(surge_RRDF)).^2).*S';
S_heave_CAPED = ((abs(heave_CAPED)).^2).*S';
S_heave_RRDF  = ((abs(heave_RRDF)).^2).*S';
S_sway_CAPED  = ((abs(sway_CAPED)).^2).*S';
S_sway_RRDF   = ((abs(sway_RRDF)).^2).*S';
S_roll_CAPED  = ((abs(roll_CAPED)).^2).*S';
S_roll_RRDF   = ((abs(roll_RRDF)).^2).*S';
S_pitch_CAPED = ((abs(pitch_CAPED)).^2).*S';
S_pitch_RRDF  = ((abs(pitch_RRDF)).^2).*S';
S_yaw_CAPED   = ((abs(yaw_CAPED)).^2).*S';
S_yaw_RRDF    = ((abs(yaw_RRDF)).^2).*S';
S_m_t_CAPED_v_1 = ((abs(m_t_CAPED_v_1)).^2).*S';
S_m_t_CAPED_v_2 = ((abs(m_t_CAPED_v_2)).^2).*S';
S_m_t_CAPED_h_1 = ((abs(m_t_CAPED_h_1)).^2).*S';
```

```
S_m_t_CAPED_h_2 = ((abs(m_t_CAPED_h_2)).^2).*S';
S_m_t_RRDF_v_1  = ((abs(m_t_RRDF_v_1)).^2).*S';
S_m_t_RRDF_v_2  = ((abs(m_t_RRDF_v_2)).^2).*S';
S_m_t_RRDF_h_1  = ((abs(m_t_RRDF_h_1)).^2).*S';
S_m_t_RRDF_h_2  = ((abs(m_t_RRDF_h_2)).^2).*S';
S_m_trolley_angle_v_1 = ((abs(m_trolley_angle_v_1)).^2).*S';
S_m_trolley_angle_v_2 = ((abs(m_trolley_angle_v_2)).^2).*S';
S_m_trolley_angle_v_twist = ((abs(m_trolley_angle_v_twist)).^2).*S';
S_m_trolley_angle_v_average = ((abs(m_trolley_angle_v_average)).^2).*S';
S_m_trolley_distance_h_1 = ((abs(m_trolley_distance_h_1)).^2).*S';
S_m_trolley_distance_h_2 = ((abs(m_trolley_distance_h_2)).^2).*S';
%
% Integral initializations
%
S_surge_CAPED_i = 0;
S_surge_RRDF_i  = 0;
S_heave_CAPED_i = 0;
S_heave_RRDF_i  = 0;
S_sway_CAPED_i  = 0;
S_sway_RRDF_i   = 0;
S_roll_CAPED_i  = 0;
S_roll_RRDF_i   = 0;
S_pitch_CAPED_i = 0;
S_pitch_RRDF_i  = 0;
S_yaw_CAPED_i   = 0;
S_yaw_RRDF_i    = 0;
S_m_t_CAPED_v_1_i = 0;
S_m_t_CAPED_h_1_i = 0;
S_m_t_RRDF_v_1_i  = 0;
S_m_t_RRDF_h_1_i  = 0;
S_m_trolley_angle_v_1_i = 0;
S_m_trolley_distance_h_1_i = 0;
S_m_t_CAPED_v_2_i = 0;
```

```
S_m_t_CAPED_h_2_i = 0;
S_m_t_RRDF_v_2_i  = 0;
S_m_t_RRDF_h_2_i  = 0;
S_m_trolley_angle_v_2_i = 0;
S_m_trolley_distance_h_2_i = 0;
S_m_trolley_angle_v_twist_i = 0;
S_m_trolley_angle_v_average_i = 0;
%
% Integral S(w)*|RAO(w)|^2
%
for i=2:1:NF,
   avg_value=0.5*(S_surge_CAPED(i)+S_surge_CAPED(i-1));
   S_surge_CAPED_i = S_surge_CAPED_i+avg_value*abs(w(i-1)-w(i));
   avg_value=0.5*(S_surge_RRDF(i)+S_surge_RRDF(i-1));
   S_surge_RRDF_i  = S_surge_RRDF_i+avg_value*abs(w(i-1)-w(i));
   avg_value=0.5*(S_heave_CAPED(i)+S_heave_CAPED(i-1));
   S_heave_CAPED_i = S_heave_CAPED_i+avg_value*abs(w(i-1)-w(i));
   avg_value=0.5*(S_heave_RRDF(i)+S_heave_RRDF(i-1));
   S_heave_RRDF_i  = S_heave_RRDF_i+avg_value*abs(w(i-1)-w(i));
   avg_value=0.5*(S_sway_CAPED(i)+S_sway_CAPED(i-1));
   S_sway_CAPED_i  = S_sway_CAPED_i+avg_value*abs(w(i-1)-w(i));
   avg_value=0.5*(S_sway_RRDF(i)+S_sway_RRDF(i-1));
   S_sway_RRDF_i   = S_sway_RRDF_i+avg_value*abs(w(i-1)-w(i));
   avg_value=0.5*(S_roll_CAPED(i)+S_roll_CAPED(i-1));
   S_roll_CAPED_i  = S_roll_CAPED_i+avg_value*abs(w(i-1)-w(i));
   avg_value=0.5*(S_roll_RRDF(i)+S_roll_RRDF(i-1));
   S_roll_RRDF_i   = S_roll_RRDF_i+avg_value*abs(w(i-1)-w(i));
   avg_value=0.5*(S_pitch_CAPED(i)+S_pitch_CAPED(i-1));
   S_pitch_CAPED_i = S_pitch_CAPED_i+avg_value*abs(w(i-1)-w(i));
   avg_value=0.5*(S_pitch_RRDF(i)+S_pitch_RRDF(i-1));
   S_pitch_RRDF_i  = S_pitch_RRDF_i+avg_value*abs(w(i-1)-w(i));
   avg_value=0.5*(S_yaw_CAPED(i)+S_yaw_CAPED(i-1));
   S_yaw_CAPED_i   = S_yaw_CAPED_i+avg_value*abs(w(i-1)-w(i));
```

```
avg_value=0.5*(S_yaw_RRDF(i)+S_yaw_RRDF(i-1));
S_yaw_RRDF_i   = S_yaw_RRDF_i+avg_value*abs(w(i-1)-w(i));
%
% Calculations for point "1"
%
avg_value=0.5*(S_m_t_CAPED_v_1(i)+S_m_t_CAPED_v_1(i-1));
S_m_t_CAPED_v_1_i = S_m_t_CAPED_v_1_i+avg_value*abs(w(i-1)-w(i));
avg_value=0.5*(S_m_t_CAPED_h_1(i)+S_m_t_CAPED_h_1(i-1));
S_m_t_CAPED_h_1_i = S_m_t_CAPED_h_1_i+avg_value*abs(w(i-1)-w(i));
avg_value=0.5*(S_m_t_RRDF_v_1(i)+S_m_t_RRDF_v_1(i-1));
S_m_t_RRDF_v_1_i = S_m_t_RRDF_v_1_i+avg_value*abs(w(i-1)-w(i));
avg_value=0.5*(S_m_t_RRDF_h_1(i)+S_m_t_RRDF_h_1(i-1));
S_m_t_RRDF_h_1_i = S_m_t_RRDF_h_1_i+avg_value*abs(w(i-1)-w(i));
avg_value=0.5*(S_m_trolley_angle_v_1(i)+S_m_trolley_angle_v_1(i-1));
S_m_trolley_angle_v_1_i = S_m_trolley_angle_v_1_i+...
   avg_value*abs(w(i-1)-w(i));
avg_value=0.5*(S_m_trolley_distance_h_1(i)+S_m_trolley_distance_h_1(i-1));
S_m_trolley_distance_h_1_i = S_m_trolley_distance_h_1_i+...
   avg_value*abs(w(i-1)-w(i));
%
% Calculations for point "2"
%
avg_value=0.5*(S_m_t_CAPED_v_2(i)+S_m_t_CAPED_v_2(i-1));
S_m_t_CAPED_v_2_i = S_m_t_CAPED_v_2_i+avg_value*abs(w(i-1)-w(i));
avg_value=0.5*(S_m_t_CAPED_h_2(i)+S_m_t_CAPED_h_2(i-1));
S_m_t_CAPED_h_2_i = S_m_t_CAPED_h_2_i+avg_value*abs(w(i-1)-w(i));
avg_value=0.5*(S_m_t_RRDF_v_2(i)+S_m_t_RRDF_v_2(i-1));
S_m_t_RRDF_v_2_i = S_m_t_RRDF_v_2_i+avg_value*abs(w(i-1)-w(i));
avg_value=0.5*(S_m_t_RRDF_h_2(i)+S_m_t_RRDF_h_2(i-1));
S_m_t_RRDF_h_2_i = S_m_t_RRDF_h_2_i+avg_value*abs(w(i-1)-w(i));
avg_value=0.5*(S_m_trolley_angle_v_2(i)+S_m_trolley_angle_v_2(i-1));
S_m_trolley_angle_v_2_i = S_m_trolley_angle_v_2_i+...
   avg_value*abs(w(i-1)-w(i));
```

```
    avg_value=0.5*(S_m_trolley_distance_h_2(i)+S_m_trolley_distance_h_2(i-1));
    S_m_trolley_distance_h_2_i = S_m_trolley_distance_h_2_i+...
        avg_value*abs(w(i-1)-w(i));
%
    avg_value=0.5*(S_m_trolley_angle_v_twist(i)+S_m_trolley_angle_v_twist(i-1));
    S_m_trolley_angle_v_twist_i = S_m_trolley_angle_v_twist_i+...
        avg_value*abs(w(i-1)-w(i));

avg_value=0.5*(S_m_trolley_angle_v_average(i)+S_m_trolley_angle_v_average(i-1));
    S_m_trolley_angle_v_average_i = S_m_trolley_angle_v_average_i+...
        avg_value*abs(w(i-1)-w(i));
    end
%
% RMS values
%
    RMS_surge_CAPED(ibeta,iHS)= sqrt(S_surge_CAPED_i);
    RMS_surge_RRDF(ibeta,iHS) = sqrt(S_surge_RRDF_i);
    RMS_heave_CAPED(ibeta,iHS)= sqrt(S_heave_CAPED_i);
    RMS_heave_RRDF(ibeta,iHS) = sqrt(S_heave_RRDF_i);
    RMS_sway_CAPED(ibeta,iHS) = sqrt(S_sway_CAPED_i);
    RMS_sway_RRDF(ibeta,iHS)  = sqrt(S_sway_RRDF_i);
    RMS_roll_CAPED(ibeta,iHS) = sqrt(S_roll_CAPED_i);
    RMS_roll_RRDF(ibeta,iHS)  = sqrt(S_roll_RRDF_i);
    RMS_pitch_CAPED(ibeta,iHS)= sqrt(S_pitch_CAPED_i);
    RMS_pitch_RRDF(ibeta,iHS) = sqrt(S_pitch_RRDF_i);
    RMS_yaw_CAPED(ibeta,iHS)  = sqrt(S_yaw_CAPED_i);
    RMS_yaw_RRDF(ibeta,iHS)   = sqrt(S_yaw_RRDF_i);
    RMS_m_t_CAPED_v_1(ibeta,iHS) = sqrt(S_m_t_CAPED_v_1_i);
    RMS_m_t_CAPED_h_1(ibeta,iHS) = sqrt(S_m_t_CAPED_h_1_i);
    RMS_m_t_RRDF_v_1(ibeta,iHS)  = sqrt(S_m_t_RRDF_v_1_i);
    RMS_m_t_RRDF_h_1(ibeta,iHS)  = sqrt(S_m_t_RRDF_h_1_i);
    RMS_m_trolley_angle_v_1(ibeta,iHS) = sqrt(S_m_trolley_angle_v_1_i);
    RMS_m_trolley_distance_h_1(ibeta,iHS) = sqrt(S_m_trolley_distance_h_1_i);
```

```
        RMS_m_t_CAPED_v_2(ibeta,iHS)  = sqrt(S_m_t_CAPED_v_2_i);

        RMS_m_t_CAPED_h_2(ibeta,iHS)  = sqrt(S_m_t_CAPED_h_2_i);

        RMS_m_t_RRDF_v_2(ibeta,iHS)   = sqrt(S_m_t_RRDF_v_2_i);

        RMS_m_t_RRDF_h_2(ibeta,iHS)   = sqrt(S_m_t_RRDF_h_2_i);

        RMS_m_trolley_angle_v_2(ibeta,iHS) = sqrt(S_m_trolley_angle_v_2_i);

        RMS_m_trolley_distance_h_2(ibeta,iHS) = sqrt(S_m_trolley_distance_h_2_i);

        RMS_m_trolley_angle_v_twist(ibeta,iHS) = sqrt(S_m_trolley_angle_v_twist_i);

        RMS_m_trolley_angle_v_average(ibeta,iHS)                            =
sqrt(S_m_trolley_angle_v_average_i);

    end

end

%

figure(1)

[th,r]=meshgrid((0:beta_incr:360)*pi/180,0.5:0.5:30);

[X,Y]=pol2cart(th,r);

h=polar(th,r);delete(h);

hold on

c_p=[0.0:0.1:2.0];

contour(X',Y',RMS_m_trolley_angle_v_average*180/pi,c_p),caxis([0 2]),colorbar

title('RMS value of Trolley Angle (deg)')

%

figure(2)

[th,r]=meshgrid((0:beta_incr:360)*pi/180,0.5:0.5:30);

[X,Y]=pol2cart(th,r);

h=polar(th,r);delete(h);

hold on

c_p=[0.0:0.1:2.0];

contour(X',Y',RMS_m_trolley_angle_v_twist*180/pi,c_p),caxis([0 2]),colorbar

title('RMS value of Trolley Twist (deg)')
```

THIS PAGE INTENTIONALLY LEFT BLANK

LIST OF REFERENCES

1.   United States Marine Corps, MAGTF Planner's Reference Manual (MAGTF Staff Training Program (MSTP) Pamphlet 5-0.3), Quantico, VA: MSTP Center, MCCDC, pp. 122 – 126, April 2001.

2.   Motion Analysis of a Trolley Interface for Ship-to-Ship Cargo Transfer, Lieutenant Brian Higgins, U.S. Coast Guard, December 2002.

3.   Experimental Study on Reduced Ramp Stress Levels Using "Smart" Damping, G. Yang et. al.

4.   Structural Dynamics: An Introduction to Computer Methods, John Wiley & Sons, Craig, R. Jr., 1981.

THIS PAGE INTENTIONALLY LEFT BLANK

INITIAL DISTRIBUTION LIST

1. Defense Technical Information Center
    Ft. Belvoir, Virginia

2. Dudley Knox Library
    Naval Postgraduate School
    Monterey, California

3. Fotis A. Papoulias
    Naval Postgraduate School
    Monterey, California

4. Chong-Ann Teh
    Naval Logistics Department, HQ Republic of Singapore Navy
    Republic of Singapore